Metabolic Engineering 69 (2022) 98–111

Contents lists available at ScienceDirect

Metabolic Engineering

journal homepage: www.elsevier.com/locate/meteng

Directed evolution of biofuel-responsive biosensors for automated optimization of branched-chain alcohol biosynthesis

Maximilian O. Bahls, Lukas Platz [1], Gaspar Morgado, Gregor W. Schmidt, Sven Panke [*]

Department of Biosystems Science and Engineering, ETH Zurich, Switzerland

ARTICLE INFO

Keywords:
AlkS
Biosensors
Branched-chain higher alcohols (BCHA)
Directed evolution
High-throughput screening

ABSTRACT

The biosynthesis of short-chain alcohols is a carbon-neutral alternative to petroleum-derived production, but strain screening operations are encumbered by laborious analytics. Here, we built, characterized and applied whole cell biosensors by directed evolution of the transcription factor AlkS for screening microbial strain libraries producing industrially relevant alcohols. A selected AlkS variant was applied for *in situ* product detection in two screening applications concerning key steps in alcohol production. Further, the biosensor strains enabled the implementation of an automated, robotic platform-based workflow with data clustering, which readily allowed the identification of significantly improved strain variants for isopentanol production.

1. Introduction

Synthetic biology and systems metabolic engineering hold the promise of sustainable production of transportation fuels and chemical building blocks from renewable feedstocks (Gustavsson and Lee, 2016; Liu and Nielsen, 2019; Straathof et al., 2019). Such bio-based production processes have the potential to reduce the reliance on limited fossil resources and to critically improve the CO_2 balance of the chemical and transportation industry, as urgently required for tackling anthropogenic climate change (Choi et al., 2020; Das et al., 2020; Wang et al., 2017).

Biofuels naturally produced by microbial cell factories include ethanol (*Saccharomyces cerevisiae* (Nissen et al., 2000)) and n-butanol (in acetone-butanol-ethanol fermentation (Nguyen et al., 2018)). Branched-chain higher alcohols (BCHAs) have superior physicochemical properties in gasoline blends (Cheon et al., 2016; Peralta-Yahya et al., 2012) and are closer to the properties required for aviation fuel. Here, isopentanol is of particular interest (Cann and Liao, 2010), as simple subsequent processing allows the production of blending agents for Jet-A1 fuel (Donnelly et al., 2016). However, BCHAs are naturally bioproduced in low concentrations and mixtures only (Hazelwood et al., 2008), and high-titer bio production of defined BCHA requires metabolically engineered host organisms (Blombach and Eikmanns, 2011; Lamsen and Atsumi, 2012). Multiple hosts including *Bacillus subtilis* (Li et al., 2011; Nielsen et al., 2009) and *B. megaterium* (Boock et al., 2019), *Corynebacterium glutamicum* (Blombach et al., 2011; Vogt et al., 2016), *Escherichia coli* (Connor and Liao, 2008; George et al., 2015; Zhang et al., 2008), *Pseudomonas putida* (Nielsen et al., 2009; Nitschel et al., 2020), *Synechocystis* PCC 6803 (Miao et al., 2018), and *S. cerevisiae* (Avalos et al., 2013; Hammer et al., 2020) were genetically modified in order to produce branched-chain C_4-alcohols such as isobutanol (2-methylpropan-1-ol) or C_5-alcohols such as isopentanol (3-methylbutan-1-ol) and isoprenol (3-methylbut-3-en-1-ol). However, rapid and cost-efficient screening tools for large strain libraries are still a key limiting factor for achieving economically competitive bioprocesses through design-build-test-learn (DBTL) cycles (Dietrich et al., 2010; Rogers et al., 2016). Biosensor-based screening workflows have gained particular interest (Binder et al., 2012) as they are faster and cheaper to run than traditional chemical analyses for biofuels based on gas- and liquid-chromatography methods, have a lower environmental footprint (Jessop, 2016), and are compatible with commercially available automation and high-throughput equipment as well (Morgan et al., 2016; Zhang et al., 2021). This advantage is of particular importance for biofoundries, which are providing an integrated infrastructure for accelerating DBTL cycles based on automation, liquid handling robots and artificial intelligence (Carbonell et al., 2020; Hillson et al., 2019).

Biosensor capacity is encoded by genetic circuits which allow to report product concentrations *in vivo* and *in situ* by conversion into fluorescent signals, which can easily be measured with established high-throughput assays (van der Meer and Belkin, 2010). This conversion is typically based on a transcription factor (TF), which recognizes the

* Corresponding author.
E-mail address: sven.panke@bsse.ethz.ch (S. Panke).
[1] current affiliation: Institute of Pharmaceutical Sciences, University of Freiburg, Germany.

https://doi.org/10.1016/j.ymben.2021.10.014
Received 5 August 2021; Received in revised form 21 October 2021; Accepted 31 October 2021
Available online 10 November 2021

product of interest and subsequently triggers expression of a fluorescent protein in a concentration-dependent fashion (Bahls et al., 2017; Mannan et al., 2017). To the best of our knowledge, only a single TF has been described so far for short-chain alcohol recognition in bacteria. The relatively uncharted σ^{54}-dependent BmoR regulator of *Thauera butanovorans* (Kurth et al., 2008; Sayavedra-Soto et al., 2005) can trigger transcription from its cognate promoter P_{BMO} was used for growth-based n-butanol titer detection (Dietrich et al., 2013). A similar system was used for screening of a small random mutagenesis library of *E. coli* for isobutanol production (Yu et al., 2019b) as well as for BmoR engineering, resulting in TF variants with reduced butanol affinity (Yu et al., 2019a). Given the diversity of targeted fuel molecules, there is a clear requirement for more biosensors.

To this end, we started from the positive transcription factor AlkS (MalT/LuxR family, 882 amino acid residues) of *P. putida* GPo1 (Canosa et al., 2000; Eggink et al., 1988; Fennewald et al., 1979; Kok et al., 1989; Moreno et al., 2009; van Beilen et al., 2001; Yuste and Rojo, 2001) and its cognate promoter P_{alkB} (Makart et al., 2007; Martinez-Garcia et al., 2020; Panke et al., 1999), originating from oil-degrading organisms (Eggink et al., 1988; Rojo, 2009; van Beilen et al., 2004) (see also Table S1). AlkS-based biosensors are well described for the detection of middle-chain n-alkanes (C_5 to C_{10} (Call et al., 2016; Calles et al., 2019; Jaspers et al., 2001; Reed et al., 2012; Sevilla et al., 2015; Sticher et al., 1997)) and were suggested to recognize the corresponding alcohols to some extent as well (Grund et al., 1975). As there are no crystal structures of the protein available, we aimed for engineering the inducer specificity (Beggah et al., 2008; Galvao and de Lorenzo, 2006) by directed evolution, characterized the resulting biosensor variants in detail, and applied one of the variants in highly automated screenings to improve isopentanol production from a defined substrate or directly from glucose.

2. Materials and methods

2.1. Materials and chemicals

If not stated otherwise, all chemicals including short DNA oligomers were purchased from Sigma Aldrich (Buchs, Switzerland), DNA isolation and purification kits from Macherey-Nagel (Dueren, Germany) or Zymo Research (Irvine, CA, USA), enzymes from New England Biolabs (Ipswich, MA, USA) and DNA fragments from IDT (Coralville, IA, USA). PCRs were carried out using high-fidelity Phusion or Q5 polymerases and the sequences of DNA parts were verified by Sanger sequencing at Microsynth (Balgach, Switzerland).

2.2. Bacterial strains, media, and cultivation conditions

In general, all cultivation and cloning procedures followed standard molecular biology protocols (Sambrook and Russel, 2001) and suppliers' recommendations. A red fluorescent derivative of *E. coli* NEB 10β (the strains used in this study are summarized in Table S3) was constructed by replacing the allose operon (*alsRBACEK*) with the gene for a constitutively expressed red fluorescent protein (λP_L:*mCherry,* see Fig. S23) by λ-red based recombineering (Datsenko and Wanner, 2000). Unless stated otherwise, the resulting *E. coli* 10β(*mCherry*) strain was used for all DNA cloning procedures, AlkS library screenings and biosensor characterizations. *E. coli* DH5α was used for KivD library screening experiments and *E. coli* BW25113 for all other alcohol production experiments. *E. coli* strains were transformed with DNA by electroporation with a micropulser (Bio-Rad, Hercules, CA, USA) at 1.8 kV and cuvettes with a 1 mm gap (Cell Projects, Harrietsham, UK). For cloning procedures and precultures Lysogeny Broth (Sambrook and Russel, 2001) (LB) was used (Becton Dickinson, Franklin Lakes, NJ, USA). If not stated otherwise, all other experiments were conducted in M9 mineral medium (Sambrook and Russel, 2001) (pH 7.4 adjusted with NaOH) supplemented with 4 g L^{-1} glucose, 20 mg L^{-1} thiamine and 100 μL L^{-1} of trace element solution US* (Panke et al., 1999). For *E. coli* 10β (*mCherry*) a leucine-isoleucine-valine (LIV) amino acid mix (Jeschek et al., 2016) was added. For combinatorial library screening and alcohol production in 96-well or 24-well plates, M9-based production medium was prepared with either 4 g L^{-1} or 5 g L^{-1} glucose and 1.25 g L^{-1} yeast extract. For solid media plates 15 g L^{-1} agar was added (Applichem, Darmstadt, Germany). Antibiotics were used, where appropriate, at the following concentrations: 100 μg mL^{-1} carbenicillin, 25 μg mL^{-1} chloramphenicol, 50 μg mL^{-1} kanamycin, 10 μg mL^{-1} gentamycin, and 50 μg mL^{-1} streptomycin. LB cultures were routinely cultivated at 37 °C, 220 rpm, and mineral medium cultures at 30 °C, 220 rpm. Culture volumes occupied 20% of the nominal volume for cultivation tubes and 10% for Erlenmeyer flasks unless stated otherwise. Cultivations in deep well plates (96-well or 24-well format) were carried out in a miniaturized fermentation system (Duetz and Witholt, 2004) (EnzyScreen, Hemsteede, The Netherlands) with a shaking amplitude of 50 mm at 300 rpm (LT-X, Kuhner, Birsfelden, Sitzerland). For induction and alcohol production experiments plates were sealed with aluminium foil or clear peelable heat seals, or screw-cap tubes and flasks were used in order to prevent alcohol evaporation. Cells were kept at 4 °C for short term storage and as cryostocks with 20% (v/v) glycerol at −80 °C otherwise.

2.3. Construction of sensor plasmids

All plasmids used in this study are summarized in Table S3. DNA oligonucleotides and other DNA sequences synthesized are listed in Tables S4 and S5, respectively. Selected plasmid maps are shown in Fig. S24. To construct the sensor-input plasmid, a low-copy number plasmid harboring the gene for the transcriptional regulator AlkS under its natural promoter P_{alkS} was constructed by PCR amplification of the corresponding region with primers AL1 and AL2 from pESM7 (Makart et al., 2007) and ligation into pCK01 (Fernandez et al., 1995) using EcoRI and HindIII sites, resulting in pCK01_P_{alkS}_*alkS* (pSC101 *ori*, CmR). Constitutive promotor variants (sequences obtained from Anderson promoter collection (accessed 01.02.2021)) for *alkS* expression were inserted by two-fragment isothermal assembly (ITA) with synthesized DNA fragment BBa_J231xx_alkS and a pCK01_P_{alkS}_*alkS* fragment PCR-amplified with primers pCK01_J231XX_alkS_fwd and pCK01_J231XX_alkS_rev, fully replacing the P_{alkS} promoter. A negative control plasmid pCK01_empty_cargo was constructed by EagI and SacI double digest of pCK01_P_{alkS}_*alkS* and self-ligation of the plasmid backbone, which removed a 3.4 kb DNA stretch including P_{alkS}:*alkS*. In general, template plasmid DNA in PCR-based procedures was digested with DpnI when appropriate.

The sensor output plasmid was constructed by exchanging the origin of replication of pSEVA231 (Martinez-Garcia et al., 2020) for that of pBR322 obtained from pRK793 (Kapust et al., 2001) by restriction with AscI and FseI and subsequent ligation. The pBR322 fragment was PCR amplified with primers pBR322_for-AscI and pBR322_rev-FseI. Next, a promoterless version of sfGFP (incl. RBS) was inserted within EcoRI and PacI sites of the multiple cloning site. The corresponding DNA fragment containing sfGFP was PCR-amplified from pET28_sfGFP (Sandia Biotech, Albuquerque, NM, USA) with SG_fwd and SG_rev prior to restriction and ligation. The P_{alkB} sequence was inserted upstream of *sfgfp* by ligation within SpeI and EcoRI sites, resulting in plasmid pAB_P_{alkB}_*sfgfp*_KanR (pBR322/rop *ori*, KanR). The DNA fragment containing the promoter sequence was obtained as the long DNA oligomer PalkB, made double stranded with the oligonucleotide PalkB_rev and Q5 DNA polymerase treatment before restriction. For screening experiments with BW25113 Δ*ilvE* (Baba et al., 2006), the KanR resistance of pAB_P_{alkB}_*sfgfp*_KanR was changed to AmpR by two-fragment ITA with PCR fragments of pAB_P_{alkB}_*sfgfp*_KanR (with primers pSEVA_abR_exchange_bb_fwd and pSEVA_abR_exchange_bb_rev) and pSEVA181 (with primers pSEVA_abR_exchange_AbR_fwd and pSEVA_abR_exchange_AbR_rev).

2.4. AlkS libraries: mutagenesis, screening, and analysis

AlkS variants were constructed by error-prone PCR (epPCR) amplification of *alkS* with primers AlkS_fwd_Gibson and AlkS_rev_Gibson, which generated a fragment that excluded the start codon as well as a putative C-terminal DNA binding domain (see Fig. S1). The epPCR was run with Taq polymerase, unbalanced concentrations of dNTPs (Fromant et al., 1995) (0.35 mM dATP, 0.4 mM dCTP, 0.2 mM dGTP, 1.35 mM dTTP), 0.05 mM Mn^{2+}, 2.95 mM Mg^{2+} and 60 ng of pCK01_P_{alkS}_*alkS* template DNA per 50 μL reaction for 30 cycles. The template DNA was linearized with MscI and NcoI prior to PCR (leading to the loss of a 38 bp fragment in the gene for CmR and thus preventing simple regeneration of the source vector by religation). The *alkS* plasmid-library was constructed by two-fragment ITA with the epPCR *alkS* part and a PCR-amplified pCK01_P_{alkS}_*alkS* backbone fragment (with primers AlkS_fwd_Gibson_backbone and AlkS_rev_Gibson_backbone, here the template DNA was linearized with AatII and EcoRV, Δ48 bp in *alkS*). The *alkS* plasmid library was used to transform *E. coli* 10β(*mCherry*) and plasmid DNA was purified from pooled cfu. The library consisted of approximately $8.1*10^4$ variants stored at −20 °C. For FACS-based screening, *E. coli* 10β(*mCherry*) [pAB_P_{alkB}_*sfgfp*_KanR] was transformed with the *alkS* library and recovered for 1 h in SOC medium (Sambrook and Russel, 2001) ($1.5*10^5$ re-transformants). Subsequently, LB with antibiotics was added to the culture for additional 2 h followed by centrifugation (3500 rcf, 4 °C, 10 min). The cell pellet was resuspended in M9 medium with 0.2 g L^{-1} glucose and cultured for 16 h. This culture was diluted ten-fold in fresh M9 medium with 4 g L^{-1} glucose, split into separate cultures and incubated for 3 h before target alcohols were added at 10 mM for additional 3 h of incubation. Next, the cells were washed twice with PBS (pH 7.4; Thermo Fisher Scientific, Waltham, MA, USA) and diluted to an OD_{600} of 0.02 (BioPhotometer D30, Eppendorf). For two rounds of enrichment (Becton Dickinson Influx Sorter), cells were sorted into LB and after 2 h of incubation the medium was changed by centrifugation and subsequent re-suspension in defined medium with 0.2 g L^{-1} glucose, subsequently repeating the workflow as described above. During the third enrichment sorting, cells were spotted on LB agar plates in 384-well format (Omintray single well plates, Thermo Fisher Scientific). Briefly, the gates for selecting alive cells were based on perpendicular forward scattering (FSCPerp) vs side scattering (polygon-shaped gate, selecting the overall cell population) as well as FSCPerp vs trigger pulse width (rectangle-shaped gate, selecting single cells). For enrichment of functional biosensor variants, gating was based on the sfGFP fluorescence signal (excitation wavelength of 488 nm and emission measured with a 530/30 nm band pass filter), while mCherry was used as a biomass marker (561 nm and 610/20 nm band pass filter). In each screening round approximately 10^7 events were recorded (about 100-fold oversampling of library sizes) and the most fluorescent cells were enriched (<0.2% of total population), followed by increasingly restrictive gating (see Fig. S3 for details of the gating strategy).

Single cfu of the sorted libraries were re-grown in LB (500 μL in deep well plates, 10 h) and subsequently diluted in defined medium (2.5% (v/v) inoculum, 750 μL, 14 h). For fluorescence measurements, cells were re-inoculated in defined medium (4% (v/v) inoculum, 500 μL) and after 2 h of incubation 250 μL of fresh medium with or without 0.3% (v/v) of alcohols was added (i.e. 0.1% (v/v) in the culture). After 6 h of induction, 200 μL samples were taken in micro-titer plates (Greiner Cellstar, Kremsmuenster, Austria) and the optical density was measured at 600 nm (OD_{600}) as well as green fluorescence at 488 nm with a 530/20 nm filter (sfGFP) and red fluorescence at 579 nm with a 616/20 nm filter (mCherry). If necessary, samples were diluted in PBS to fit the linear measurement range of the plate reader (Tecan M1000 Pro, Maennedorf, Switzerland).

The *alkS* sequences of the input plasmid of the top-performing biosensor constructs were subsequently sequenced including the upstream RBS and promoter region (nine *alkS* variants for n-butanol, six for isopentanol, four for isobutanol, as well as the parental wild-type). For Sanger sequencing of each *alkS* variant four primers were used (pAlkS_fwd_1, pAlkS_fwd_2, pAlkS_fwd_3, and pAlkS_fwd_4). The *alkS* sequences were aligned with the ones of the natural OCT plasmid (NCBI GenBank AJ245436) and five additional expression plasmids containing the *alkS* sequence (AJ299427, AF118921, AJ302087, AJ414668, and AJ302086) using Clustal Omega 1.2.4 (Sievers et al., 2011) (via EMBL-EBI web service). Note that in the parental *alkS* sequence we found bases C1228A (Q410K), C1392G (T464T), and T2568C (H856H) mutated as compared to the *alkS* sequence of the OCT plasmid (AJ245436).

For PCR-based single site-directed *alkS* mutagenesis at amino acid residues K183, A375, S377, S379, L401, and Q410, primers with NNK codons at the corresponding DNA positions were used (AlkS_QC_*residue*_NNK_fwd and AlkS_QC_*residue*_NNK_rev, e.g. AlkS_QC_K183_NNK_fwd and AlkS_QC_K183_NNK_rev for residue K183) and applied to template plasmid pCK01_P_{alkS}_*alkS*. *E. coli* 10β(*mCherry*) [pAB_P_{alkB}_*sfgfp*_KanR] was transformed with the individual libraries and single cfu were transferred to deep well plates and evaluated as described above (>90 cfu per site). For isobutanol, two additional rounds of evolution were conducted as described above but with more restrictive FACS-gating conditions and a negative pre-enrichment round to remove variants with a high basal biosensor output (Fig. S3). The second epPCR library was created based on pCK01_P_{alkS}_*alkS*_T1135C (coding for S379P, size of $1.2*10^5$ variants and $1.6*10^5$ re-transformants). Site-directed mutagenesis and variant evaluation was carried out at positions K115+A117, T336, R355, and T591 using primers AlkS_QC_*residue*_NNK_fwd and AlkS_QC_*residue*_NNK_rev with pCK01_P_{alkS}_*alkS*_T1135C as template. The third epPCR library was created based on pCK01_P_{alkS}_*alkS* _A1006T_G1064A_T1135C (coding for T336S, R355H, S379P, $5.1*10^5$ variants and $5.8*10^6$ re-transformants). Amino acid specific site-directed mutagenesis and variant evaluation was carried out as described above for D17E, I19V, R110G, V171L, V376L, and R397G using primers AlkS_*residue*_fwd and AlkS_*residue*_rev with template pCK01_P_{alkS}_*alkS* _A1006T_G1064A_T1135C.

2.5. Single-cell biosensor characterization and AlkS structure modeling

In general, the selected biosensor variants were cultivated in deep well plates and analyzed in a plate reader as described above. For initial biosensor circuit characterization the cells were incubated with alcohols for 6 h and in all other experiments for 16 h. Additional single cell data was obtained from diluted cultures (OD_{600} of 0.05 in PBS) with a Beckman Coulter Cytoflex S (Brea, CA, USA) or a Becton Dickinson LSRFortessa for fitting of biosensor transfer functions. The sfGFP fluorescence was measured at an excitation wavelength of 488 nm and emission with a 525/40 nm or 530/30 nm band pass filter, respectively. All cultivations were carried out in biological triplicates unless stated otherwise. Gating was based on forward scattering area (FSC-A) vs side scattering area (SSC-A, polygon-shaped gate, selecting the overall cell population) as well as side scattering height (SSC–H) vs SSC-A (rectangle-shaped gate, selecting single cells). Samples for alcohol analysis were taken before addition to the biosensor culture and after 16 h of incubation. For all alcohols we observed neither chemical impurities nor significant conversion or degradation during the cultivations (Fig. S11). For single cell data evaluation and visualization FlowJo software was used (FlowJo LLC, Ashland, OR, USA). Transfer functions were fitted with a non-linear regression model as four-parameter dose-response curves (Prism 8.4.2, GraphPad, San Diego, CA, USA) and Z' values as described previously (Zhang et al., 1999) (more details are available in Fig. S10). The AlkS mutations corresponding to the characterized biosensor variants were mapped to a structural model based on the crystal structure of a signal transduction ATPase of *Pyrococcus horikoshii* (UniProtKB O58663, 3.40 Å resolution) created with the Phyre2 web tool (Kelley et al., 2015) (72% sequence coverage with 100% confidence).

2.6. KivD SSM library screening for isopentanol production by whole-cell conversion

The parental plasmid p631_*araC*_P_{BAD}_*kivDyqhD* was created in two steps from pIPO2 (Nitschel et al., 2020). First, an *araC*_P_{BAD}_*kivD_yqhD_alsS_ilvC_ilvD* fragment was PCR-amplified from template pIPO2 with primers p_AvrII_araC_isoalcohol_forward and p_NotI_araC_isoalcohol_reverse, digested with AvrII and NotI and subsequently ligated into the multiple cloning site of pSEVA631 cut open with the same enzymes, resulting in p631_*araC*_P_{BAD}_isobutanol. Second, the *alsS_ilvC_ilvD* part was removed by PCR amplification of a corresponding DNA fragment with primers pkivD_yqhD_NheI_fwd and pkivD_yqhD_NheI_rev using p631_*araC*_P_{BAD}_isobutanol as template. This fragment was subsequently cut with NheI and self-ligated, resulting in p631_*araC*_P_{BAD}_*kivDyqhD* (for a more detailed overview of the plasmids, see Table S3). For PCR-based SSM at KivD amino acid position V461 primers pkivD_V461X_fwd and pkivD_V461X_rev were used (NNK codon) with plasmid p631_*araC*_P_{BAD}_*kivDyqhD* as template. For V461A and V461D mutations primers kivD_V461A_fwd and kivD_V461A_rev or kivD_V461D_fwd and kivD_V461D_rev were used, respectively. The corresponding 20 plasmids encoding the full SSM library as well as an empty plasmid control (pSEVA631) were used for transformation of the sensor strain *E. coli* DH5α [pCK01_P_{alkS}_*alkS*_L401G; pAB_P_{alkB}_*sfgfp*_KanR]. The screening was carried out as described for single-cell biosensor characterization, but 0.2% (v/v) substrate (4-methyl-2-oxopentanoic acid) and 0.2% (w/v) L-arabinose were added concomitantly to the cultures instead of alcohol (percentages represent final amounts in the culture). Samples for optical measurements and product analysis were taken after 20 h of incubation. The crystal structure of KdcA (PDB 2VBF) was used in order to visualize the conserved active center of KivD (Miao et al., 2018) with PyMOL 3.2.3 (Schrodinger, New York, NY, USA).

2.7. Isoalcohol pathways and combinatorial library for isopentanol production

For genomic pathway integration, an *araC*_P_{BAD}_*kivD_yqhD_alsS_ilvC_ilvD* fragment was amplified from pIPO2 with primers p_araC_ISO2_fwd_NheI and p_araC_ISO2_rev_NotI and integrated into a pBG fragment via restriction and ligation. The pBG fragment was amplified from pBG14g (Zobel et al., 2015) with primers pTn7_upstream_NotI_fwd and pTn7_rev_NheI. The resulting pBG_*araC*_P_{BAD}_isobutanol plasmid was co-transformed with pTNS2 for genomic integration in three different *E. coli* strains: 10β(*mCherry*), BW25113, and BW25113 Δ*ilvE* (Baba et al., 2006). For *E. coli* BW25113 Δ*ilvE* the KanR resistance cassette was removed with pCP20 as described previously (Cherepanov and Wackernagel, 1995). The correct insertion of the isobutanol pathway as well as KanR removal were verified by whole genome NGS (Novogene, Cambridge, UK). *E. coli* PIR2 was used for pBG plasmid (*ori* R6K) cloning and maintenance.

For creation of p221_*araC*_P_{BAD}_*leuABCD* the *leuABCD* operon of *E. coli* BW25113 was amplified with primers pleuABCD_pBAD_fwd and pleuABCD_MCS_rev from genomic DNA, *araC*_P_{BAD} (incl. RBS) was amplified from pNG413.1 (Nitschel et al., 2020) with primers pBAD_MCS_fwd and pBAD_leuABCD_rev, and pSEVA221 was digested with KpnI and SalI. The corresponding DNA parts were assembled by three-fragment ITA (also see Table S3 for an overview of plasmids).

For combinatorial *leuA* library generation by restriction and ligation, first p221_*araC*_P_{BAD}_*leuABCD* template DNA was amplified with primers p221_araC_Pbad_blunt_fwd and p221_araC_Pbad_KpnI_rev. The synthetic combinatorial *leuA* library fragment with an NGGANG in the RBS consensus motif and a degenerate NNK codon for position V462 (1.5 kb; GeneArt, Thermo Fischer Scientific) was amplified with primers pleuA_GeneArt_KpnI_short_fwd and pGeneART_leuA_lib_rev. The primers for blunt-end ligation were phosphorylated with T4 polynucleotide kinase prior to PCR (p221_araC_Pbad_blunt_fwd and pGeneART_leuA_lib_rev).The two fragments were separately digested with KpnI and subsequently combined by ligation. This library DNA was used for transformation of *E. coli* 10β(*mCherry*), cfu were pooled, plasmid DNA isolated, and then stored as a plasmid library pool ($1.0*10^5$ transformants). The distribution of the individual degenerate library parts in the plasmid pool was check by NGS (Novogene, Cambridge, UK; Fig. S22).

The plasmid library pool was used for transformation of *E. coli* BW25113 Δ*ilvE* gISO2 [pCK01_P_{alkS}_*alkS*_L401G pAB_P_{alkB}_*sfgfp*_AmpR] and the resulting *E. coli* BW25113 Δ*ilvE* gISO2 biosensor strain library cultured on agar plates (total of $6.0*10^4$ transformants). The correct assembly of library plasmids was check by cPCR with primers pIP_seq_araC_rev and pPBAD_rev with *Taq* DNA polymerase. The corresponding PCR product (634 bp) was cut with KpnI (260 bp + 374 bp) in order to distinguish the library plasmid from the template plasmid (no KpnI site). Translation initiation rates for RBS were predicted per web-based RBS Calculator (Salis et al., 2009) accessed via DeNovoDNA (State College, PA, USA.).

2.8. Automation-based high-throughput screening of combinatorial library

Single cfu of the *E. coli* BW25113 Δ*ilvE* gISO2 biosensor strain library (described above) were first cultured in 384-well master plates in LB medium (30 °C, 350 rpm, 16 h) and subsequently replicated in M9-based production medium additionally supplemented with 0.2% (w/v) L-arabinose for induction and actual screening (30 °C, 350 rpm, 20 h). Plates were closed with peelable, clear heat seals to prevent evaporation (PlateLoc thermal sealer; Agilent, Santa Clara, CA, USA). All steps run on a customized automation-platform based on two EVO200 robots (Tecan) are described in more detail below. Biosensor measurements after the final incubation were carried out with a plate reader as described above. The obtained raw data was directly used for k-means clustering with R (Team, 2014) (version 4.0.3) and the number of clusters determined by plotting the ratio of "within sum of squares/between sum of squares" (Thorndike, 1953) (see Fig. S20). Briefly, the algorithm of Hartigan and Wong was used (Hartigan and Wong, 1979), with three clusters (cluster = 3) and twenty random starts (nstart = 20). For ggplot2-based data visualization, the factoextra R package was used. Strain variants obtained from all clusters were re-grown from the master cultures on LB agar plates, single cfu cultured in deep well plates (n = 3) and subsequently diluted in M9 production medium with 0.2% (w/v) L-arabinose as described above. After 24 h cell densities and biosensor outputs were measured as well as samples taken for metabolite analysis. The full workflow is shown in Fig. S18. For Sanger sequencing of the degenerate library sites a corresponding DNA fragment was amplified by colonyPCR with primers pIP_seq_araC_rev and pGeneART_leuA_lib_rev and subsequently sequenced with primers pBAD-for and pFP14_leuABCD_2.

2.9. Automated colony picking

For robotic handling, agar plates were prepared in Omnitray single well plates with a lid. For reliable colony picking, the agar inside the plates had to be perfectly level and without a meniscus at the edges. This was achieved by adhering to the following protocol. LB agar was autoclaved and allowed to cool to approximately 60 °C before antibiotics were added. An aliquot of 40 mL of was added to each plate using a serological pipette. The plates were covered with lids and left for 1 h at room temperature to allow the agar to solidify. To dry the plates, they were left without lid under a laminar flow hood for 30 min. Plates were stored inside a plastic bag at 4 °C until further use. The *E. coli* BW25113 Δ*ilvE* gISO2 biosensor strain library was plated at an average density of 280 cfu per plate, corresponding to 2.5 cfu per cm^2. Colony picking was performed on a Tecan EVO 200 robotic platform, controlled by the EVOware standard software (Tecan). Inputs to the colony picking method were provided using a custom Excel input sheet. The platform

was equipped with a Pickolo colony picking module (SciRobotics Ltd., Kfar Saba, Israel) consisting of a light table, camera and software. The Pickolo module was used to take images of the agar plates and identify the positions of the colonies. A custom image processing script, implemented in Fiji (Schindelin et al., 2012), was used to correct the images of the agar plates for uneven illumination before identification of colonies. To ensure picking of single colonies, the minimum distance between colonies was set to approximately 2 mm. The robotic platform was equipped with a liquid displacement pipetting system using ultrapure water as system liquid. The pipetting system featured eight stainless steel fixed tips connected to 2500 µL dilutors, and two tip wash stations. Before pipetting media or picking of colonies, the tips were decontaminated as follows. The tips were rinsed from the inside (3 mL) and outside (4 mL) in wash station one. Volumes of 2500 µL (when pipetting media) or 200 µL (when picking colonies) of 2% sodium hypochlorite solution were aspirated from a 100 mL trough (Tecan) into each tip and incubated for 10 s. The hypochlorite solution was then dispensed back into the 100 mL trough. To clear the tips of residual hypochlorite solution they were rinsed from the inside (3 mL) and outside (4 mL) in wash station two. To contain the microbe containing aerosols that emerge during use of the wash stations, the wash stations were equipped with a custom made lid. The lid was manufactured from acrylic sheets using a laser cutter. Colonies were picked into clear 384-well F-bottom plates (Greiner). Each well of the plates was automatically filled with 40 µL of LB media before colony picking started. For picking, 20 µL of media was aspirated into a freshly decontaminated tip, the tip was brought in contact with the colony, and the cells transferred to the 384-well plate by dispensing 20 µL. To ensure that no cross-contamination occurred during colony picking process, 24 wells in each plate were not inoculated with a colony and served as negative control wells. The platform allowed picking of about 200 colonies per hour, and up to 1440 colonies were picked without user interaction in a single run. All method files, the design files of the wash station lid, the Pickolo colony picking profile (*.prf file) and the Excel input sheet are available online from github (https://github.com/gregorwschmidt/tecan-colonypickingandcounting).

2.10. Automated replication of libraries into fresh media

Replication of the picked libraries into fresh media was performed on a Tecan EVO 200 robotic platform, controlled by the EVOware standard software. The robotic platform was equipped with a liquid displacement pipetting system using ultrapure water as system liquid. The pipetting system featured eight teflon-coated fixed tips connected to four 1000 µL and four 50 µL dilutors, and two tip wash stations. Before pipetting media, the tips were decontaminated with 2% sodium hypochlorite as described above. The platform was additionally equipped with a PCR cycler (Biometra TRobot, Analytik Jena, Jena, Germany). Transfer of master cultures into screening cultures was achieved using a 96-pin replicator (Scinomix, Earth City, MO, USA). First, all wells of the screening plates (black 384-well clear F-bottom plates, Greiner) were automatically filled with 60 µL production media using the pipetting system of the robot. Then, cells were transferred by dipping the 96-pin replicator first into the master plate and then into the screening plates using the robotic manipulator arm of the system. To replicate a single 384-well plate four distinct pin replication steps were necessary. Between pin replication steps, the 96-pin replicator was decontaminated as follows. Using the robotic manipulator arm of the system, the pin replicator was dipped into an Omnitray plate filled with 70 mL of 2% hypochlorite solution. The pin replicator was moved inside the hypochlorite solution for 20 s to facilitate washing. Two more wash steps in ultrapure water and 95% ethanol were performed in the same fashion. Then, the pin replicator was placed inside a skirted 96-well PCR plate (FrameStar, 4titude Ltd., Surrey, UK) which was located in the PCR cycler and preheated to 80 °C. The pin replicator was left to dry inside the heated PCR plate for at least 3 min, before it was used for the next replication step. Replication of four 384-well master plates into four 384-well screening plates with the automated method took 1.8 h. All method files and the Excel input sheet are available online from github (https://github.com/gregorwschmidt/tecan-libraryreplication). Details and images of the crucial automation steps are available in Fig. S19.

2.11. Isopentanol production strains and cultivation in deep well plates

For curing of the biosensor plasmids (but not the p221_ *araC*_P_{BAD}_*leuABCD*$_{max}$ plasmid variant with AGGAGG consensus motif and V462F), the best performing isopentanol strain obtained from the screen was cultivated in LB supplemented with kanamycin at 42 °C for 16 h. The plasmid DNA was isolated and used for transformation of *E. coli* 10β (*mCherry*). The re-isolated p221_ *araC*_P_{BAD}_*leuABCD*$_{max}$ plasmid was subsequently used as the template for PCR-based mutagenesis, introducing either a weak RBS (plasmid p221_ *araC*_P_{BAD}_*leuABCD*$_{weakRBS}$) or back-mutation to V462V at the FBR site (p221_ *araC*_P_{BAD}_*leuABCD*$_{noFBR}$). For the corresponding PCRs, primers leuA_weak_RBS_fwd and leuA_weak_RBS_rev or leuA_G462_fwd and leuA_G462_rev were used, respectively. Next, the three different p221_ *araC*_P_{BAD}_*leuABCD* variants where used for separate transformation of *E. coli* BW25113 Δ*ilvE* gISO2. The resulting strains as well as the parental isobutanol production strain were cultivated in 2 mL of LB in deep well plates in 24-square well format for 10 h and re-inoculated in 2 mL M9-based production medium (5% (v/v) inoculum) for 16 h (n = 4). These precultures were diluted to an OD_{600} of 0.2 in 2 mL of the same medium but supplemented with 0.2% (w/v) L-arabinose and the plates sealed with aluminum foil. Samples for metabolite and glucose analysis were taken after 20 h of cultivation.

2.12. Metabolite and glucose analysis

For quantitative alcohol determination in deep well plate experiments in 96-well format 700 µL of each sample were spun down (21,130 rcf, 4 °C, 10 min) and 500 µL of the culture supernatant were diluted in 500 µL water. In experiments in 24-well format, 2 mL of each sample were spun down and 1 mL of undiluted supernatant used. Next, 100 µL of internal standard solution (1% (v/v) n-pentanol in water) was added and the sample briefly vortexed, except for qualitative alcohol analysis experiments during biosensor characterization (Fig. S11). Subsequently 500 µL methyl tert-butyl ether (SupraSolv, Merck, Darmstadt, Germany) was added and the mixture thoroughly vortexed. If necessary, samples were briefly centrifuged for complete phase separation. For gas chromatography (GC) analysis, 400 µL of the organic phase were transferred into glass vials closed with PTFE snap-caps (Wicom, Maienfeld, Switzerland). The GC system consisted of a 6890N GC-FID with a 7683 auto-sampler and a DB-WAX UI capillary column (30 m with 0.25 mm diameter; all Agilent) with helium as the carrier gas (2 mL min^{-1}; PanGas, Dagmersellen, Switzerland). Samples were injected in splitless mode with a volume of 1 µL. The temperature of the injector and the FID were maintained constant at 225 °C and 250 °C, respectively. The oven temperature was initially held at 40 °C for 5 min. Next, the temperature was increased to 120 °C at a rate of 15 °C min^{-1}, followed by heating to 230 °C at a rate of 50 °C min^{-1} and held constant for 4 min. For glucose analysis, 500 µL undiluted supernatant samples in snap cap vials were analyzed on an HPLC system (Agilent 1200, 10 µL injection per sample) with a refractive index detector and a Metab-AAC column (30 cm × 7.8 mm, 10 µm particle size; Insera, Dueren, Germany) at 40 °C using an isocratic protocol (5 mM H_2SO_4 as mobile phase, flow of 600 µL min^{-1}). Concentrations were determined by extrapolation from standard curves based on samples of diluted pure compounds.

3. Results

3.1. Design and construction of an AlkS-based biosensor circuit for alcohol detection

In order to convert the presence of alcohol in water into a rapidly detectable signal such as fluorescence, we placed the expression of a fluorescent reporter protein (sfGFP) under the control of P_{alkB} on a medium-copy number plasmid (*ori* pBR322/*rop*). AlkS was expressed under the control of its natural promoter P_{alkS} from a low-copy plasmid (*ori* pSC101). Additionally, we tested three commonly used constitutive promoters of varied strengths (see Fig. 1). When we added 10 mM n-pentanol (C_5), which is the shortest straight chain functional alkane inducer known for AlkS (Stricher et al., 1997), all designs produced a fluorescent response, indicating a certain flexibility of the system with respect to *alkS* expression. The concentration of the inducer was chosen based on previous screening efforts (Yu et al., 2019a) and the fact that most short-chain alcohols do not display massive toxicity at this level.

Still, the biosensor performance depended significantly on the details of the AlkS expression. The low expression strength promoter J23117 significantly limited the maximum biosensor output. Using the natural P_{alkS}, which enables a positive-negative feedback loop (Canosa et al., 2000), allowed tight control, as indicated by low basal sfGFP output, and high maximum induction level. While using the strong constitutive promoter J23100 led to a similarly high fluorescence output, this design showed a non-desirable high basal output. Using the medium strength promoter J23106 generated a circuit behavior similar to the circuit with P_{alkS} but a higher basal and a lower maximum output. Thus, we continued with the P_{alkS}::*alkS*/P_{alkB}::*sfgfp* system, which showed its largest fold-change of around 55-fold 6 h after induction.

Finally, we checked the homogeneity of the biosensor response to 10 mM n-pentanol at single cell level. The sfGFP output of the biosensor strain population increased homogeneously and almost completely (97%), indicating that under these conditions induction was nearly comprehensive and therefore n-pentanol mass transfer across the membrane not limiting. Additionally, in the absence of AlkS (empty plasmid control) and the presence of n-pentanol no biosensor response was observed, indicating that AlkS is essential for this response. As expected from literature, sensor output was only observed for n-pentanol and no response was found in the presence of the shorter C_4 straight-chain alcohol n-butanol.

3.2. Directed evolution of AlkS and characterization of expanded alcohol detection

Next, we used the P_{alkS}::*alkS*/P_{alkB}::*sfgfp*-based biosensor circuit for evolving AlkS for the recognition of smaller and sterically more demanding alcohols than n-pentanol. As shown in Fig. 2, we generated a variant library by epPCR-based random mutagenesis of the regulator's gene sequence. Based on an alignment with the well-characterized MalT regulator of *E. coli*, the C-terminal domain of AlkS likely contains a helix-turn-helix motif responsible for binding to the cognate P_{alkB}-promoter DNA and this part was excluded from mutagenesis (see Fig. S1). The *alkS* variants obtained were reintroduced in the sensor circuit and used for transformation, resulting in a biosensor strain library with approximately 10^5 members. On average, we found in the library immediately after construction about 5.5 amino acid residues exchanged per AlkS variant (7.6 bases exchanged per gene, 28% silent mutations, based on Sanger sequencing of ten *alkS* genes corresponding to a sequence total of approximately 26 kb). In addition, and as expected, we did not find any mutated bases outside of the designed random mutagenesis area. We also observed the bias known for error-prone PCR libraries (Drummond et al., 2005), i.e. a preference for mutating A or T and overall more transitions than transversions (Zhao et al., 2014).

From simple qualitative plate experiments we found that about 29% of the variants remained inducible with n-pentanol or were constitutively in the on-state (Fig. S2). The rest of the library was analyzed by flow cytometry, which allows for suitable library member oversampling (in our experiments, typically 50 to 100-fold). The sensor-strain library was cultivated in separate batches supplemented with 10 mM of either n-butanol, isobutanol, or isopentanol. The most fluorescent fractions of the corresponding populations were enriched by three consecutive rounds of cultivation in the presence of alcohol followed by fluorescence assisted cell sorting (FACS, for details on populations and gating see Fig. S3). Next, we verified that sorted populations were indeed enriched in alcohol-inducible biosensor variants and excluded variants that showed high basal sfGFP output (exemplarily shown for the sorting conducted with n-butanol, Fig. 2B. For all sorted batches see Fig. S4).

We readily found eight different AlkS variants responsive to n-butanol, three variants responsive to isopentanol and a single variant responsive to isobutanol. On average, after enrichment 3.5 amino acid residues had been exchanged per AlkS variant. As we did not expect all random mutations to be beneficial or optimal for expanded alcohol detection, we identified mutations that had been occurred in several AlkS variants and conducted site-saturation mutagenesis in the parental AlkS on these sites. Mutations and selected target-sites are summarized in Tables 1 and S2, respectively.

Among the AlkS variants responsive to n-butanol, position L401 was changed in two independent variants, and this position was found to be quite flexible:

When screening an NNK-site saturation library of position 401, we could retrieve 15 different AlkS variants (401I, M, N, Q and W-variants

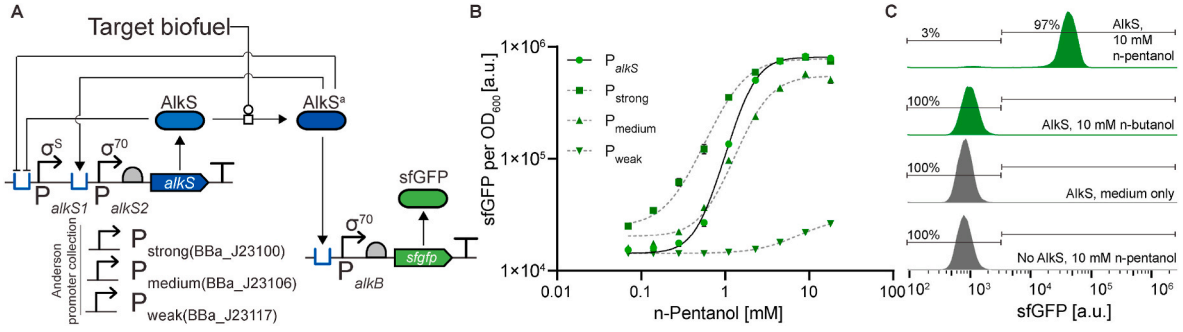

Fig. 1. Design and characterization of AlkS-based biosensor circuits. (**A**) Genetic circuit map for biofuel detection including a small promoter library for *alkS* expression. For simplicity, the sequence containing the two regulatory regions of $P_{alkS1/2}$ is usually referred to as P_{alkS}. The constitutive promoters fully replaced the whole P_{alkS} promoter. (**B**) Dose-response curves of *E. coli* sensor strain with different promoter variants (data points are means with standard deviation, lines indicate Hill fits of means, all $R^2 \geq 0.99$, n = 3). (**C**) Biosensor response for C_4 (n-butanol) and C_5 (n-pentanol) straight-chain alcohols with the circuit using the P_{alkS} promoter upstream of *alkS* (flow cytometer, >35`000 events per population). No AlkS: same plasmid as in AlkS-experiment but without *alkS* gene; medium only: no alcohol added to the medium. AlkS^a, activated AlkS; Bba_x, BioBrick part name; sfGFP, superfolder green fluorescent protein.

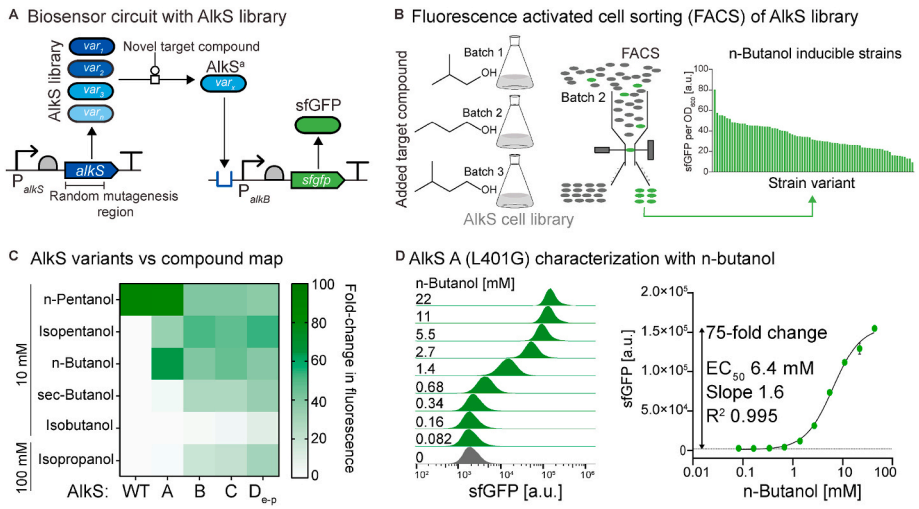

Fig. 2. Directed evolution of transcription factor AlkS for small- and branched-chain alcohol detection and biosensor characterization. (**A**) Scheme of the biosensor genetic circuit, including the part of AlkS that experienced random mutagenesis (amino acids 2–821). (**B**) Representative FACS-based enrichment of alcohol responsive AlkS mutants (batch 1, isobutanol; batch 2, n-butanol (data shown); batch 3, isopentanol). (**C**) Overview of alcohol induction profiles of AlkS variants (flow cytometer, >100'000 events per population, mean of median fluorescence, n = 3). (**D**) Representative single-cell dose-response of a biosensor strain with AlkS A and the corresponding transfer function with n-butanol (>100'000 events per population, line indicates Hill fit of means of median fluorescence, error-bars represent standard deviations, dotted line indicates mean basal sfGFP fluorescence, n = 3). Abbreviations: AlkS[a], activated AlkS regulator.

Table 1
Overview of AlkS variants found in FACS-based screening of error-prone *alkS* strain libraries. For rounds two and three of screening for isobutanol inducible AlkS variants, parentheses indicate the parental mutations. Mutation Q410K of wild-type (WT) AlkS is not listed again for mutant variants. For additional details, see Table S2.

AlkS variant	Amino acids exchanged
WT	Q410K
for **n-Butanol**	1) A463T, G753R 2) V11D, D40E, L401S, L469H 3) M103K, A117V, S379P, L542Q 4) R50K, A375T, F538L, Q767R 5) K183I, L401S 6) Y302F, S377G, S627G, V653I 7) I31V, K451N, K595R 8) K183R, E267V, I300V, Y307F, Q390L
Isopentanol	1) P10L, C47S, A375V, E504Q 2) M103K, A117V, S379P, L542Q 3) R50K, A375T, F538L, Q767R
Isobutanol	1.1) M103K, A117V, S379P, L542Q 2.1) R355H, (S379P), T591A 2.2) E102G, K115T, T336S, (S379P) 2.3) (S379P), V513M, E567G, L580V 3.1) D17E, I19V, R110G, V171L, (T336S), (R355H), V376L, (S379P), R397G

were not retrieved), and of these 15 only three (L401L, F and P) did not show a response to n-butanol.

In particular, AlkS L401G (abbreviated as AlkS "A") showed the most improved sensor output. Encouragingly, it also maintained a low basal output in the absence of inducer (Figs. S5 and S6).

Screening an NNK-library of position K183, which also had appeared in two variants, did not result in AlkS variants with an improved induction profile for n-butanol.

For isopentanol and isobutanol, all identified AlkS variants showed either an A375 V/T or an S379P mutation. From NNK-screens on the two sites, we confirmed the variant with the mutation S379P (AlkS "B") as the variant with the best response to those alcohols, while variants with exchanges at A375 showed similarly improved induction with isopentanol but no significant improvement for isobutanol.

Form this first epPCR library, we identified AlkS mutants that worked well for the short chain n-butanol and the branched chain isopentanol, but only to a smaller extent for the branched isobutanol. Hence, we conducted two additional rounds of evolution for improving the response to isobutanol. The second round, now based on error-prone replication using AlkS S379P as the template and again followed by site saturation mutagenesis for characterization of the impact of promising sites, lead to the further improved variant AlkS T336 R355H S379P ("C"). Finally, the third round, based on epPCR of the gene of variant C, led to the identification of two variants: "D" (AlkS T336 R355H S379P R397G), which showed an improved biosensor output for sec-butanol (butan-2-ol, see below) and "$D_{e\text{-}p}$" (AlkS D17E I19V R110G V171L T336 R355H V376L S379P R397G), which showed an improved dynamic range for isobutanol.

Next, we tested the new biosensor strains synthesizing the defined AlkS variants (parent, A, B, C, $D_{e\text{-}p}$) against a diverse panel of C_3 to C_5 alcohols to characterize the inducer specificity (see Fig. 2C and Fig. S7). As expected, the parental AlkS biosensor showed sfGFP output only for n-pentanol, with a change in fluorescence of about 85-fold. For the A variant, we found strong induction with n-butanol (64-fold) and isopentanol (about 30-fold). However, no induction with the other alcohols including isobutanol was observed, a feature utilized later for the screening of strain libraries. For the B variant we observed strong induction with isopentanol (50-fold) as well as n-butanol (40-fold) and sec-butanol (28-fold). Besides, this AlkS variant showed some inducibility with isobutanol (about 3-fold). For variants C and $D_{e\text{-}p}$, the output with isobutanol improved further to 5-fold and 10-fold, respectively. We were curious whether also isopropanol would give a response with those variants that responded to isobutanol, but found only a very weak or no response. Given that isopropanol has a much reduced toxicity for *E. coli* than all the other tested alcohols, we resorted to testing higher isopropanol concentrations, and indeed found a 30 fold-increase of fluorescence AlkS $D_{e\text{-}p}$ in the presence of 100 mM isopropanol. We completed the biosensor characterization by determining the full transfer functions (fit to Hill curves, all R^2 >0.93, Fig. 2D, full data in Figs. S8–S11) for the best-in-class biosensors and their cognate alcohols (Table 2).

In summary, the biosensor variants showed maximum fold-changes between 20- and 80-fold with EC_{50} concentrations in the range of 5–30 mM and Z' scores >0.7, which indicates excellent suitability for screening (Dietrich et al., 2013; Zhang et al., 1999). The fold-changes in sensor output were smaller for alcohols with shorter C-chains as well as sterically more demanding methyl side chains or C–C double bonds. This reduction resulted mainly from increased basal sensor output of the corresponding AlkS variants, while the maximum output stayed similar to, or even increased above, the maximum wild-type sensor output with n-pentanol (Fig. S10). In addition, all biosensor variants were still inducible with n-pentanol.

Table 2
Biosensor performance characteristics for evolved AlkS variants and the corresponding target compounds. EC_{50}: half maximal effective concentration; n: slope (or Hill coefficient, a measure of sensitivity); † alcohol concentration at which the sensor response value for fold-change was determined, growth was severely affected at higher alcohol concentrations tested; Z': effectiveness of the circuit for high-throughput screens (Zhang et al., 1999), generally, Z'-values above 0.5 are considered sufficient for an effective screening assay (Dietrich et al., 2013), also, the concentration at which the Z'-value was computed is given. For dose-response curves and parameter calculation see Fig. S10.

Compound	AlkS mutant (abbreviation)	EC_{50} [mM]	n	Max. fold-change, concentration [mM]†	Z', conc. [mM]
n-Pentanol	wild-type (WT)	3.9	1.8	86, 18.4	0.98, 9.2
n-Butanol	L401G (A)	6.4	1.6	75, 43.8	0.94, 11
Isopentanol	S379P (B)	9.8	0.95	29, 9.2	0.84, 4.6
Isoprenol	S379P (B)	7.2	1.3	21, 39.4	0.95, 39.4
sec-Butanol	(B) + T336S, R355H, R397G (D)	28.9	0.86	48, 87.6	0.94, 43.8
Isobutanol	(D) + D17E, I19V, R110G, V171L V376L ($D_{e\text{-}p}$)	12.4	2.0	19, 43.2	0.71, 43.2

3.3. Biosensor-based isopentanol detection in whole-cell catalysis

So far, the alcohol that was meant for detection had always been added externally. As a next step, we verified the applicability of the biosensor circuit for detecting alcohols produced *in vivo*. Isopentanol was chosen as the target product for its outstanding physico-chemical properties suitable for bio-fuel related applications. To implement isopentanol biosynthesis, we targeted the commonly used Ehrlich degradation pathway (Hazelwood et al., 2008). This pathway catalyzes the transformation of various 2-keto acids, precursors in amino acid biosynthesis, to products such as isopentanol and isobutanol (Lamsen and Atsumi, 2012). To disentangle the signals for the two possible products, we selected AlkS variant A (L401G) for the biosensor, as it responded well to isopentanol but hardly to isobutanol (Fig. 2C and Fig. S13).

First, we added only two enzymes to *E. coli*, specifically the enzymes for the final steps of Ehrlich degradation (see Fig. 3): KivD (an α-ketoisovalerate decarboxylase of *Lactococcus lactis*) and YqhD (a NADPH-dependent aldehyde reductase of *E. coli*). To enable isopentanol formation, the corresponding 2-keto acid substrate 4-methyl-2-oxopentanoic acid was supplied to the culture medium at a concentration of 0.2% (v/v). As expected, the expression of the two enzymes, from a bicistronic operon under the control of an L-arabinose inducible promoter, allowed whole-cell conversion of the 2-keto acid to isopentanol, while no product formation was observed in the absence of the operon.

Previously, the highest specific activity of KivD had been found *in vitro* for the substrate 2-ketoisovalerate (leading to isobutanol), and only a reduced relative activity for 4-methyl-2-oxopentanoic acid (leading to isopentanol) of about 23% (de la Plaza et al., 2004). However, the selectivity of KivD for larger alcohols, such as n-pentanol, was shown to improve for less bulky amino acid residues at position V461 (Chen et al., 2017), an essential residue in catalytic function (Chen et al., 2017; Zhang et al., 2008). This left the possibility that mutagenesis at site 461 might lead to a KivD variant with improved properties for isopentanol production. To this end, a KivD V461X site-saturation mutagenesis (SSM) library was generated, re-introduced into the biosensor strain, and supplied with 4-methyl-2-oxopentanoic acid. The resulting strains produced a variety of fluorescence levels, potentially indicating a variety of isopentanol-levels. Strains with different fluorescence levels were taken to validate the correlation between strain-produced isopentanol level as determined by chemical analysis and the fluorescence level resulting from the triggering of the biosensor circuit in the same cell. Over the whole range of product titers we found a good correlation between the two ($R^2 = 0.98$, see Fig. 3C). The maximum isopentanol concentration was found for wild-type KivD V461V, indicating that the parental protein was in this case the best variant. The obtained isopentanol concentration obtained in this assay was 4.4 mM, resulting in a nine-fold increase in biosensor fluorescence output, and corresponded to 27% (mol/mol) isopentanol yield from the 2-keto acid. Besides, all strain populations showed homogenously expressed sfGFP in flow cytometer analysis after whole-cell catalysis. The single cell data set also showed excellent agreement with plate reader-based measurements as used here in the following library screening workflow ($R^2 > 0.99$, see Fig. S14).

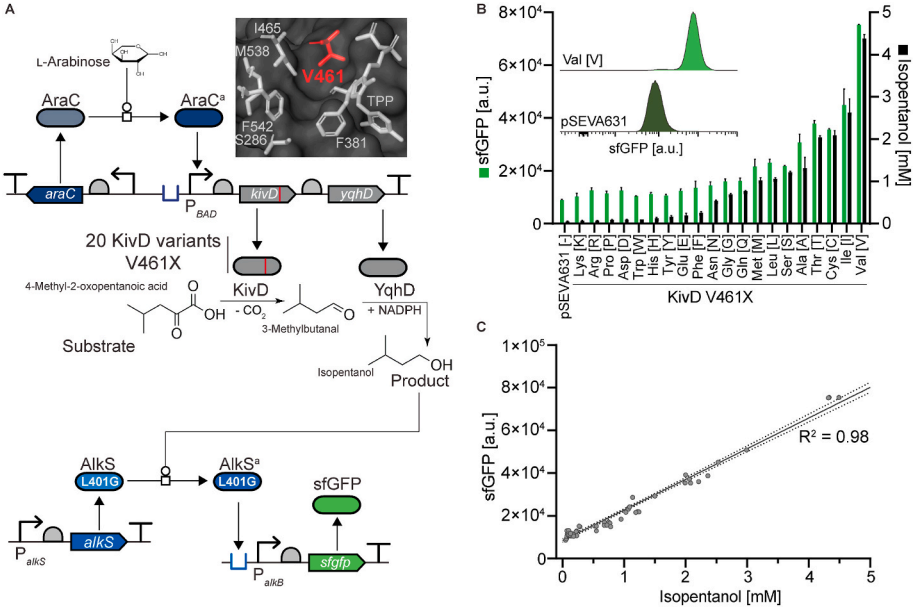

Fig. 3. Biosensor verification for production and *in situ* detection of isopentanol. (**A**) Genetic circuits for varied whole-cell transformation of a 2-keto acid substrate (4-methyl-2-oxopentanoic acid) to isopentanol by overexpression of a KivD V461X library and YqhD in combination with biosensor-based product detection. (**B**) KivD variants ranked by isopentanol titer with the corresponding biosensor fluorescence output. The inlet shows the fluorescence of representative populations for the best performing KivD V461 (Val [V]) and the negative control (pSEVA631). All flow cytometer data >100'000 events per population, means of medians with standard deviation, isopentanol titers are means with standard deviation, all n = 3). (**C**) Correlation of isopentanol product concentrations and the corresponding median biosensor fluorescence outputs (line is best-fit linear regression, dotted lines indicate the 95% confidence bands). $AlkS^a$, activated AlkS regulator; $AraC^a$, activated AraC regulator; KivD, α-ketoisovalerate decarboxylase (visualized with KdcA structure, PDB 2VBZ), sfGFP, superfolder green fluorescent protein; TPP, thiamine pyrophosphate; YqhD, alcohol dehydrogenase.

3.4. Automation-based screening of a combinatorial library for optimized BCHA biosynthesis

In order to efficiently produce branched-chain higher alcohols from glucose via the full Ehrlich degradation pathway, enzymes AlsS (α-acetolactate synthase, from *B. subtilis*) IlvC (keto-acid reductoisomerase) and IlvD (dihydroxy-acid dehydratase, both from *P. putida*) have to be overproduced in addition to KivD and YqhD (Nitschel et al., 2020). These five enzymes correspond to the pathway from pyruvate to isobutanol (Fig. 4, brown and grey), but at the same time constitute the upper part of the isopentanol pathway. In order to adjust the metabolic flux towards isopentanol, enzymes LeuA (2-isopropylmalate synthase), LeuB (3-isopropylmalate dehydrogenase), LeuC (3-isopropylmalate dehydratase large subunit), and LeuD (3-isopropylmalate dehydratase small subunit, all from *E. coli*'s leucine biosynthesis pathway) have to be overproduced as well (Fig. 4, blue). As a result, isobutanol is an unavoidable side product in isopentanol production (and vice versa, due to the essentiality of *leuABCD* (Baba et al., 2006)) in this commonly applied production route. However, the AlkS A (L401G) variant allows selective detection of isopentanol without activation by isobutanol (see Fig. 4C) and thus the detection of strains with an improved isopentanol yield $Y_{P/S}$ for a given substrate.

For the implementation of the proposed production system, we started by stable, site-specific integration (Zobel et al., 2015) of the isobutanol production operon into the genome of *E. coli* BW25113 Δ*ilvE,* which lacks the gene for a branched-chain-amino-acid aminotransferase. This knock-out improves BCHA production (Connor and Liao, 2008) by eliminating side reactions otherwise competing with KivD for shared 2-keto acid substrates (also see Fig. 4). As expected, when growing on production medium the Δ*ilvE* strain allowed improved isobutanol production (4.3 mM) as compared to the parental strain BW25113 and a common cloning strain (1.4 mM and 1.7 mM, respectively, see Fig. S15).

Next, we cloned the *leuABCD* operon on a broad-host range plasmid (*ori* pBBR1) under the control of the L-arabinose inducible *araC*/P_{BAD} system. Furthermore, the expression of the first gene in an operon can have a substantial influence on the expression of the operon (Levin-Karp et al., 2013), so we varied the translation efficiency of the first gene in the operon, *leuA*, whose gene product also catalyzes the first committed step of isopentanol production. The *leuA* RBS strength was varied with a sixteen-membered degenerate library (NGGANG (Jeschek et al., 2016)), spanning a predicted translation initiation range (TIR) of 89 to 15,023 arbitrary units. As parental LeuA is known to be limited by feed-back inhibition (Connor and Liao, 2008), we additionally randomized the LeuA amino acid position G462, a residue crucial for feedback release (FBR)) (Gusyatiner et al., 2002). To this end, a degenerate NNK sequence coding for all 20 natural amino acids (and a stop codon) was used. A plasmid-based pool of this combinatorial library was combined with the isobutanol production host equipped with the biosensor system (see Fig. 5A).

To screen for improved isopentanol producers, we developed an automated workflow using liquid handling robots and 384-well plates, which allow economic storage and handling of the variants in arrayed format. Arraying the different strain variants turned out to be important as the alcohol molecules diffuse readily across microbial membranes and therefore different strains need to remain separate from each other (Fig. S16). The workflow allowed reliable recovery of an isopentanol production strain from a mock library (Fig. S17). Briefly, the robotic system picked individual bacterial colonies (colony forming units, cfu) and transferred them into liquid cultures of 60 μL volume (throughput limiting step, about 200 cfu h^{-1}). After 16 h of incubation, these precultures were replicated into production medium by the robot. Finally, isopentanol formation was assessed by fluorescence output of the biosensor after 20 h of production time. The detailed screening schedule and the integrated automation steps are summarized in Figs. S18 and S19. The raw biosensor data obtained from the plate reader was subsequently analyzed with a k-means (Hartigan and Wong, 1979) unsupervised machine learning algorithm in order to obtain a cluster of improved strain variants, comparison of which can inform on the logic of potential production improvement, as opposed to looking at a single top performer.

For the isopentanol production library, a total of 4320 cfu were screened (see Fig. S17). This represents a thirteen-fold theoretical oversampling of the strain library. However, we found that only about 50% of the initial library cfu contained the correctly assembled combinatorial DNA fragment (16/32, by colony PCR) thus reducing the actual oversampling value to six-fold, with a 58% likelihood to have screened the full library. Based on the biosensor data, three distinct strain clusters were generated (Fig. 5B and Fig. S20). For all clusters arbitrarily selected variants were re-cultured in a deep-well plate fermentation system (Duetz et al., 2000) and evaluated in terms of biosensor output as well as BCHA titers produced. For all selected strains a clear positive correlation between isopentanol production and biosensor output was found (R^2 = 0.94, Fig. 5C). As expected from the interdependency of the isobutanol and isopentanol production pathways, this coincided with a clear negative correlation of biosensor outputs and isobutanol concentrations (R^2 = 0.95).

For two of the sensor output clusters (no. 1 and 2, cluster sizes of 277 and 3976, respectively) neither increased biosensor output nor improved isopentanol production was observed (0/6 variants), as was expected from the low mean cluster values for biosensor output. Accordingly, for two of these six variants *leuA* was completely absent, in

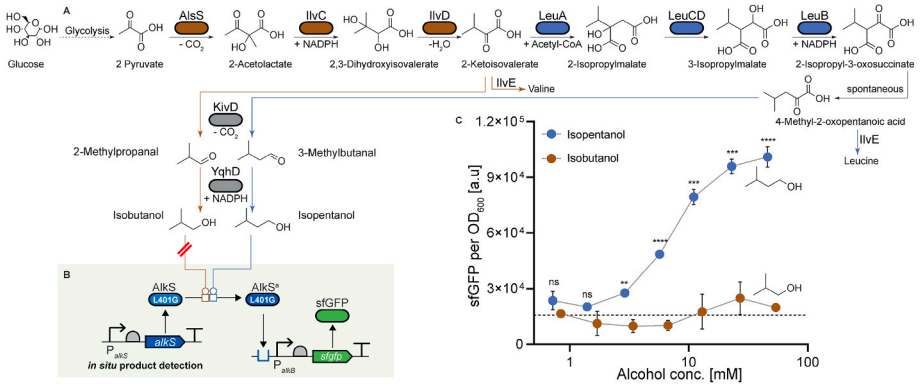

Fig. 4. Branched-chain higher alcohol biosynthesis via Ehrlich degradation and biosensor-based product detection. (**A**) Reactions and corresponding enzymes required for isobutanol and isopentanol biosynthesis. (**B**) Specific product detection *in situ* with AlkS L401G-based biosensor system. (**C**) Biosensor response for externally added isopentanol (blue, target product) and isobutanol (brown, expected side product). Data points are means with standard deviation, dotted line indicates basal sensor output without alcohol added (n = 3). Abbreviations: $AlkS^a$, activated AlkS regulator. AlsS, acetolactate synthase; $AraC^a$, activated AraC regulator; IlvC, ketol-acid reductoisomerase; IlvD, dihydroxy-acid dehydratase; KivD, α-ketoisovalerate decarboxylase; LeuA, 2-isopropylmalate synthase; LeuB, 3-isopropylmalate dehydrogenase; LeuC, 3-isopropylmalate dehydratase (large subunit); LeuD, 3-isopropylmalate dehydratase (small subunit); sfGFP, superfolder green fluorescent protein; YqhD, alcohol dehydrogenase. Multiple unpaired t-tests with P-values (biosensor output for isobutanol vs isopentanol): ns ≥ 0.05, ** 0.001 to 0.01, *** 0.0001 to 0.001, **** < 0.0001.

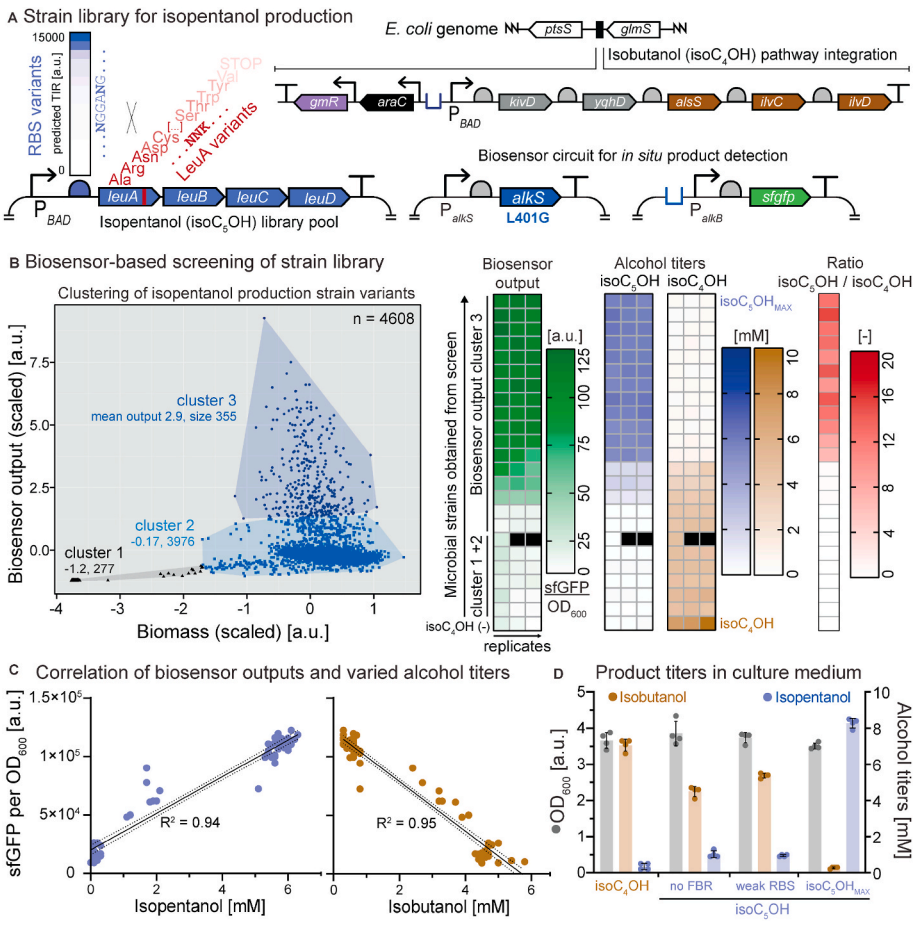

Fig. 5. Biosensor-based high-throughput library screen for improved isopentanol production strains. (**A**) Overview of combinatorial library for *leuA* expression, catalyzing the first committed step of isopentanol production, in an isobutanol production strain background equipped with the AlkS L401G biosensor system. Sixteen ribosomal binding site (RBS) variants were combined with 20 variants of *leuA* stemming from site-saturation mutagenesis at feed-back release (FBR) site G462X. (**B**) Clustering of scaled biosensor output and biomass, based on a k-means unsupervised learning algorithm. The corresponding data set was obtained from an automated screening workflow with 4320 library variants picked plus additional blank and control wells (culture volume of 60 µL, total 4608 wells). Variants of each cluster were re-assessed in terms of biosensor output and alcohol titers produced (three variants each for clusters one and two, 17 variants for cluster three; culture volume of 750 µL, black wells indicate no growth, n = 3). (**C**) Correlation of alcohol titers with biosensor fluorescence outputs for the microbial strains obtained from the screen (line is best-fit linear regression, dotted lines indicate the 95% confidence bands). (**D**) Verification of switch from isobutanol to isopentanol production with culture supernatants of the top-performing isopentanol strain ("isoC$_5$OH$_{MAX}$", TIR of 15023 a.u. and G462F) and control strains either lacking the FBR mutation (TIR of 15023 a.u. and G462G, "no FBR") or the strong RBS (TIR of 89 a.u. and G462F, "weak RBS") in comparison to the parental isobutanol production strain ("isoC$_4$OH") after 20 h cultivation at 30 °C (single data points with bar representing their mean and error-bars indicating standard deviations, n = 4). Transcription initiation rate (TIR) predicted according to (Salis et al., 2009). Abbreviations: as in Fig. 4. GmR, gentamycin resistance (gentamicin-3-acetyltransferase); RBS, ribosome binding site.

three variants frameshift mutations or deletions had occurred, while the last variant had a very low predicted TIR of 100 a.u. For the variants obtained from the cluster with highest mean sensor output (no. 3, cluster size of 355), about 90% (15/17 variants) showed increased biosensor output as well as improved isopentanol titers. In this cluster, we mainly found high predicted TIR values for *leuA* translation, while no clear pattern for the G462X sites was found except that we could not retrieve any variant with wild-type LeuA G462 (Fig. S21). Also, we verified by NGS of the full plasmid library pool that the best performing DNA sequences were not overrepresented before screening (Fig. S22). From this result we concluded that for efficient isopentanol production [i] elimination of the feed-back inhibition of *leuA* is required together with [ii] high expression strength for *leuA*.

Starting from the parental isobutanol strain producing 0.13 mM isopentanol and 8.2 mM isobutanol, the best-performing isopentanol variant "isoC$_5$OH$_{MAX}$" obtained from cluster no. 3 (RBS with AGGAGG consensus motif and a predicted TIR 15023 a.u., G462F) produced a titer of 5.8 mM isopentanol, with 0.4 mM of isobutanol as a side product. This represents a 45-fold improvement in product titer, with a molar ratio of isopentanol over isobutanol of about 13-fold. The plasmid harboring the best performing *leuABCD* operon found in the screen was re-introduced in the parental isobutanol production strain (i.e. without the biosensor system). Alternatively, we inserted into this strain one of two control plasmids, one carrying the best performing *leuABCD* operon but with a weak RBS in front of *leuA* (predicted TIR of 89 a.u.) or with the high-performing RBS but without a FBR mutation in LeuA (G462G). When growing on production medium (5 g L^{-1} glucose, 1.25 g L^{-1} yeast extract) the optimized strain produced 8.3 mM of isopentanol and 0.28 mM of isobutanol, while the two control strains produced significantly less isopentanol (0.95 mM or 1.0 mM, respectively), confirming that the combination of both high expression strength and the FBR mutation are required for high isopentanol production (see Fig. 5D).

4. Discussion

Microbial strain engineering is a key priority for enabling the sustainable production of chemical building blocks and biofuels. With ever more powerful bioengineering and DNA synthesis methods for the creation of extensive strain libraries, biosensor-based screening of such libraries becomes a focal point of synthetic biology research (Dietrich et al., 2010; Morgan et al., 2016). Biosensors can facilitate more economical and higher throughput assessments of strain library members in comparison to established chemical analysis methods. Here, directed evolution of the AlkS transcription factor allowed for the construction of genetic circuits for *in situ* detection of various BCHA, a compound group that was previously not recognized by wild-type AlkS. We identified two single residues of the total 882 amino acids constituting AlkS which are amenable for significantly expanding the inducer spectrum. It is notable that we readily identified suitable mutation, even though the number of evaluated variants reflects only a tiny fraction of possible variants. However, as quickly becomes clear from the analysis of the permissiveness of site L401, this site was easy to identify as most of the possible mutations at this site led to a butanol-responsive phenotype. Specifically, residue L401 was mutated for recognition of n-butanol as well as isopentanol and S379 for alcohols such as 2-butanol and isobutanol, while also serving as the parental template for further improved AlkS mutants harboring several mutations. All of those compounds are part of the OECD list of high production volume chemicals

(The 2007 OECD List of High Production Volume Chemicals, 2009). None of these hot-spot sites had been found previously in an effort made for improved hexane and pentane detection with AlkS variants (Reed et al., 2012).

As no protein structure is available for AlkS and only very few related regulator structures of the MalT-family were solved, it is difficult to directly map the mutated amino acids to a specific function or mechanism. We note that changes in inducer specificities usually evolve via stem forms with a more broadened (as opposed to switched) inducer specificity (Galvao et al., 2007), and we observe such behavior here as well. Recent insights into the mechanisms of signal transduction ATPases (including the transcriptional activator MalT (Lisa et al., 2019), see Figs. S1 and S12 for a corresponding AlkS structural model based on homology (Kelley et al., 2015)) might also provide an explanation why we found in our screens AlkS variants with changed specificity and high basal signal output, but also others that have changed specificity but retained low basal signal output. Briefly, the signal transduction mechanism includes a tightly controlled state, in which the sensor domain covers the core nucleotide-binding oligomerization domain (NOD). Upon first low affinity inducer binding a more open and responsive, but partially leaky, state is formed, with reduced auto-inhibitory interaction between NOD and sensor domain. Next, high-affinity inducer binding allows an ADP to ATP exchange in the NOD, which triggers formation of the active, multimeric regulator. Hence, mutations in the NOD-sensor domain interface could lead to a regulator structure with its equilibrium state shifted towards the high-affinity binding state (i.e. skipping the low-affinity binding state) and thus allowing induction with additional inducers otherwise not recognized, at the cost of a partially increased basal activity. This would be consistent with the behavior of some of the AlkS variants responsive to isobutanol (e.g. AlkS $D_{e\text{-}p}$). In contrast, mutations in the sensor domain sequence might allow for a changed inducer spectrum while maintaining the tightly controlled, autoinhibition state with basal output levels similarly low as the one found for the wild-type regulator, as seen in the present work for the n-butanol-enabling mutation L401G.

When applying one of the new biosensors to facilitate screening activities, we found in a KivD V461X library screen for isopentanol production that the targeted amino acid position is indeed crucial for 4-methyl-2-oxopentanoic acid conversion, as expected from the location of the residue in the active site pocket (Berthold et al., 2007). The wild-type valine residue performed best in whole-cell catalysis for isopentanol production, although in earlier experiments V461A had been found as optimal if the KivD substrate is larger than α-ketoisovalerate (de la Plaza et al., 2004), which is the case here. V461A had also been found in a screen for improved n-pentanol production (Chen et al., 2017). In the present experiments, such improvements were not picked up in the screen as one specific substrate was supplied at a relatively high concentration and not in competition with other high-concentration substrates originating from a common over-expression pathway. Still, and importantly, this small library screen confirmed that the biosensor system reliably ranks strain variants in agreement with the actual product titers achieved, and the corresponding fluorescence measurement takes seconds for a microtiter plate as compared to one to several hours for gas chromatography analysis (Lin et al., 2014).

For the biosensor system using AlkS L401G, significantly different sensor outputs between isobutanol and isopentanol as well as the structural isomers isobutanol and n-butanol were found, a feature that had not been found previously despite efforts to engineer BmoR (Yu et al., 2019a). This inducer-specificity is an essential feature in order to detect strains that produce isopentanol at high yields. The most common metabolic engineering approach for branched-chain higher alcohols utilizes the Ehrlich degradation pathway (Blombach and Eikmanns, 2011). As a result, isobutanol is an essentially unavoidable side product in all such metabolic engineering efforts, e.g. in *E. coli*-based BCHA production from cellulose and protein rich waste streams (Liu et al., 2017), which leads to false positive biosensor output unless the system is specific for the C_5 product. Here, we demonstrated a successful screen for improved isopentanol production without adverse false-positive sensor activation, despite starting from a parental strain producing isobutanol from a genome-integrated overexpression pathway.

In the screened combinatorial library for isopentanol production, we found high *leuA* RBS strength to be crucial for product formation, while for the FBR site G462X no clear pattern was observed. This is consistent with a previous study in which the LeuA G462D expression level was found to be crucial for isopentanol formation (Connor and Liao, 2008). Specifically, for the best performing strain obtained from the screen we found the consensus AGGAGG Shine-Dalgarno sequence, which also had the highest predicted TIR in the strain library (15023 a.u.), and an FBR mutation at G462.

The implemented automated screening system based on AlkS variants and fluorescence proved very useful in efficiently identifying strains from a library that showed improved isopentanol titers and the corresponding improved product yield on C-source. On the one hand, it allowed screening of a library of more than 4000 cfu, which is, to the best of our knowledge, amongst the largest published for biofuel-related research (Dietrich et al., 2013; Yu et al., 2019b) and could easily be extended due to the automated workflow. On the other hand and assuming a contribution of the yeast extract as determined previously (Connor and Liao, 2008), we could easily identify a maximum isopentanol titer that corresponds to a product yield on glucose of about 0.14 $g_{isoC5OH}\ g_{Glc}^{-1}$. Those results are on par with state-of-the-art metabolic engineering efforts for isopentanol production under comparable cultivation conditions (0.13 $g_{isoC5OH}\ g_{Glc}^{-1}$ for 5 g L^{-1} glucose and 5 g L^{-1} yeast extract) with an *E. coli* strain harboring a synthetic RBS for expression of LeuA (G462D) but also harboring seven additional genomic gene knock-outs as well as requiring three plasmids for pathway overexpression (Connor and Liao, 2008). Besides, the results verified that the selected cultivation conditions allowed full conversion of the C-source without reaching the product toxicity limits. However, further improvements in isopentanol titer were achieved previously with increasing the C-source concentrations (Connor and Liao, 2008) and applying antimetabolite-based screenings (Connor et al., 2010). Promising clones were finally applied in two-phase systems for product extraction, which allowed high glucose concentrations and the production of 9.5 g L^{-1} isopentanol (Connor et al., 2010).

Finally, the biosensor-based readout data sets were directly utilized for simple unsupervised learning and data clustering as desirable for automated, efficient and unbiased pattern identification in screening for high-producing strains (Lawson et al., 2021). These data clusters could readily be utilized for full computational integration of library evaluation in DBTL cycles in biofoundries for the accelerated development of industrially relevant microbial strains (Hillson et al., 2019; Zhang et al., 2021). The data clusters are also suitable for visualization of library variant distributions that simple rankings of specific fluorescence might miss due to normalization to biomass, while also allowing principle component analysis if multidimensional readouts are used (Presnell and Alper, 2019).

The developed biosensor system could be readily employed for additional tasks such as building screening and selection systems based on alternative biosensor outputs (Qian et al., 2019; Taylor et al., 2016) or dynamic feedback control and time-of-requirement expression of alcohol efflux pumps (Dunlop et al., 2010). The AlkS variants found most likely also allow for the detection of other compounds available from biosynthesis such as (gaseous) n-butane (Sheppard et al., 2016) or additional industrially relevant alcohols derived from Ehrlich degradation, e.g. phenylalcohols (Machas et al., 2017), as well as other molecule classes with a relatively straight C-chain, e.g. ketones (Mehrer et al., 2019). Besides, AlkS is known to be functional in other industrially relevant host microorganisms such as *P. putida* (Calles et al., 2019). As the majority of the molecules mentioned readily diffuse across microbial membranes, the developed sensor strains should be useful for screening

of several other product-molecule sources as well, for instance in co-cultivation schemes with organisms that are less amenable to intricate genetic circuit engineering.

Funding

European Union Project EmPowerPutida grant 635536 (MOB).

Author contributions

M.O.B. conceived and carried out the experimental work as well as data analysis. L.P. contributed to biosensor characterization and alcohol production. G. M. constructed initial biosensor plasmids and cloning strains. G. W. S developed the automation-based screening platform. M. O.B., G. W. S. and S.P. wrote the manuscript, all authors reviewed and approved the manuscript. S.P. provided the project outline, supervision and resources.

Data and materials availability

All data required for the conclusions of this article are available in the main text or the supplementary materials. Additional data related to this paper may be requested from the authors. Biosensor plasmids are available from addgene (ID 166502/3), files for automation on github (https://github.com/gregorwschmidt).

Declaration of competing interest

Authors declare that they have no competing interests.

Acknowledgments

We thank M. Otto and F. Pfeifer for help with metabolite analytics; D. Gerngross for help with automated colony picking; T. Roberts for critically reading the manuscript; S. Schmitt for help with NGS data analysis; R. Nitschel, R. Takors and Ingenza Inc. for providing plasmids pIP02 and pNG413.1; V. de Lorenzo and the members of his laboratory for providing pSEVA plasmids; S. Koebbing and L. Blank for providing pBG14g; T. Lopes and the D-BSSE Single Cell Facility for excellent assistance with FACS experiments. We are indebted to the whole EmPowerPutida project consortium for most valuable feedback and discussions.

Appendix A. Supplementary data

Supplementary data to this article can be found online at https://doi.org/10.1016/j.ymben.2021.10.014.

References

Avalos, J.L., Fink, G.R., Stephanopoulos, G., 2013. Compartmentalization of metabolic pathways in yeast mitochondria improves the production of branched-chain alcohols. Nat. Biotechnol. 31, 335-41.

Baba, T., Ara, T., Hasegawa, M., Takai, Y., Okumura, Y., Baba, M., Datsenko, K.A., Tomita, M., Wanner, B.L., Mori, H., 2006. Construction of Escherichia coli K-12 in-frame, single-gene knockout mutants: the Keio collection. Mol. Syst. Biol. 2, 2006 0008.

Bahls, M.O., Kardashliev, T., Panke, S., 2017. Novel Sensors for Engineering Microbiology (In Consequences of Microbial Interactions with Hydrocarbons, Oils, and Lipids: Production of Fuels and Chemicals), pp. 331–357.

Beggah, S., Vogne, C., Zenaro, E., Van Der Meer, J.R., 2008. Mutant HbpR transcription activator isolation for 2-chlorobiphenyl via green fluorescent protein-based flow cytometry and cell sorting. Microb Biotechnol 1, 68–78.

Berthold, C.L., Gocke, D., Wood, M.D., Leeper, F.J., Pohl, M., Schneider, G., 2007. Structure of the branched-chain keto acid decarboxylase (KdcA) from Lactococcus lactis provides insights into the structural basis for the chemoselective and enantioselective carboligation reaction. Acta Crystallogr D Biol Crystallogr 63, 1217–1224.

Binder, S., Schendzielorz, G., Stabler, N., Krumbach, K., Hoffmann, K., Bott, M., Eggeling, L., 2012. A high-throughput approach to identify genomic variants of bacterial metabolite producers at the single-cell level. Genome Biol. 13.

Blombach, B., Eikmanns, B.J., 2011. Current knowledge on isobutanol production with Escherichia coli, Bacillus subtilis and Corynebacterium glutamicum. Bioeng Bugs 2, 346–350.

Blombach, B., Riester, T., Wieschalka, S., Ziert, C., Youn, J.W., Wendisch, V.F., Eikmanns, B.J., 2011. Corynebacterium glutamicum tailored for efficient isobutanol production. Appl. Environ. Microbiol. 77, 3300–3310.

Boock, J.T., Freedman, A.J.E., Tompsett, G.A., Muse, S.K., Allen, A.J., Jackson, L.A., Castro-Dominguez, B., Timko, M.T., Prather, K.L.J., Thompson, J.R., 2019. Engineered microbial biofuel production and recovery under supercritical carbon dioxide. Nat. Commun. 10, 587.

Call, T.P., Akhtar, M.K., Baganz, F., Grant, C., 2016. Modulating the import of medium-chain alkanes in E. coli through tuned expression of FadL. J. Biol. Eng. 10, 5.

Calles, B., Goni-Moreno, A., de Lorenzo, V., 2019. Digitalizing heterologous gene expression in Gram-negative bacteria with a portable ON/OFF module. Mol. Syst. Biol. 15, e8777.

Cann, A.F., Liao, J.C., 2010. Pentanol isomer synthesis in engineered microorganisms. Appl. Microbiol. Biotechnol. 85, 893–899.

Canosa, I., Sanchez-Romero, J.M., Yuste, L., Rojo, F., 2000. A positive feedback mechanism controls expression of AlkS, the transcriptional regulator of the Pseudomonas oleovorans alkane degradation pathway. Mol. Microbiol. 35, 791–799.

Carbonell, P., Le Feuvre, R., Takano, E., Scrutton, N.S., 2020. In silico design and automated learning to boost next-generation smart biomanufacturing. Synth Biol (Oxf). 5 ysaa020.

Chen, G.S., Siao, S.W., Shen, C.R., 2017. Saturated mutagenesis of ketoisovalerate decarboxylase V461 enabled specific synthesis of 1-pentanol via the ketoacid elongation cycle. Sci. Rep. 7, 11284.

Cheon, S., Kim, H.M., Gustavsson, M., Lee, S.Y., 2016. Recent trends in metabolic engineering of microorganisms for the production of advanced biofuels. Curr. Opin. Chem. Biol. 35, 10–21.

Cherepanov, P.P., Wackernagel, W., 1995. Gene disruption in Escherichia coli - TcR and KmR cassettes with the option of Flp-catalyzed excision of the antibiotic-resistance determinant. Gene 158, 9–14.

Choi, K.R., Jiao, S., Lee, S.Y., 2020. Metabolic engineering strategies toward production of biofuels. Curr. Opin. Chem. Biol. 59, 1–14.

Connor, M.R., Cann, A.F., Liao, J.C., 2010. 3-Methyl-1-butanol production in Escherichia coli: random mutagenesis and two-phase fermentation. Appl. Microbiol. Biotechnol. 86, 1155–1164.

Connor, M.R., Liao, J.C., 2008. Engineering of an Escherichia coli strain for the production of 3-methyl-1-butanol. Appl. Environ. Microbiol. 74, 5769–5775.

Das, M., Patra, P., Ghosh, A., 2020. Metabolic engineering for enhancing microbial biosynthesis of advanced biofuels. Renew. Sustain. Energy Rev. 119.

Datsenko, K.A., Wanner, B.L., 2000. One-step inactivation of chromosomal genes in Escherichia coli K-12 using PCR products. Proc. Natl. Acad. Sci. U. S. A. 97, 6640–6645.

de la Plaza, M., Fernandez de Palencia, P., Pelaez, C., Requena, T., 2004. Biochemical and molecular characterization of alpha-ketoisovalerate decarboxylase, an enzyme involved in the formation of aldehydes from amino acids by Lactococcus lactis. FEMS Microbiol. Lett. 238, 367–374.

Dietrich, J.A., McKee, A.E., Keasling, J.D., 2010. High-throughput metabolic engineering: advances in small-molecule screening and selection. Annu. Rev. Biochem. 79, 563–590.

Dietrich, J.A., Shis, D.L., Alikhani, A., Keasling, J.D., 2013. Transcription factor-based screens and synthetic selections for microbial small-molecule biosynthesis. ACS Synth. Biol. 2, 47–58.

Donnelly, J., Horton, R., Gopalan, K., Bannister, C.D., Chuck, C.J., 2016. Branched ketone biofuels as blending agents for jet-A1 aviation kerosene. Energy Fuel. 30, 294–301.

Drummond, D.A., Iverson, B.L., Georgiou, G., Arnold, F.H., 2005. Why high-error-rate random mutagenesis libraries are enriched in functional and improved proteins. J. Mol. Biol. 350, 806–816.

Duetz, W.A., Ruedi, L., Hermann, R., O'Connor, K., Buchs, J., Witholt, B., 2000. Methods for intense aeration, growth, storage, and replication of bacterial strains in microtiter plates. Appl. Environ. Microbiol. 66, 2641–2646.

Duetz, W.A., Witholt, B., 2004. Oxygen transfer by orbital shaking of square vessels and deepwell microtiter plates of various dimensions. Biochem. Eng. J. 17, 181–185.

Dunlop, M.J., Keasling, J.D., Mukhopadhyay, A., 2010. A model for improving microbial biofuel production using a synthetic feedback loop. Syst Synth Biol 4, 95–104.

Eggink, G., Engel, H., Meijer, W.G., Otten, J., Kingma, J., Witholt, B., 1988. Alkane utilization in Pseudomonas oleovorans. Structure and function of the regulatory locus alkR. J. Biol. Chem. 263, 13400–13405.

Fennewald, M., Benson, S., Oppici, M., Shapiro, J., 1979. Insertion element analysis and mapping of the Pseudomonas plasmid alk regulon. J. Bacteriol. 139, 940–952.

Fernandez, S., de Lorenzo, V., Perez-Martin, J., 1995. Activation of the transcriptional regulator XylR of Pseudomonas putida by release of repression between functional domains. Mol. Microbiol. 16, 205–213.

Fromant, M., Blanquet, S., Plateau, P., 1995. Direct random mutagenesis of gene-sized DNA fragments using polymerase chain reaction. Anal. Biochem. 224, 347–353.

Galvao, T.C., de Lorenzo, V., 2006. Transcriptional regulators a la carte: engineering new effector specificities in bacterial regulatory proteins. Curr. Opin. Biotechnol. 17, 34–42.

Galvao, T.C., Mencia, M., de Lorenzo, V., 2007. Emergence of novel functions in transcriptional regulators by regression to stem protein types. Mol. Microbiol. 65, 907–919.

George, K.W., Thompson, M.G., Kang, A., Baidoo, E., Wang, G., Chan, L.J., Adams, P.D., Petzold, C.J., Keasling, J.D., Lee, T.S., 2015. Metabolic engineering for the high-yield production of isoprenoid-based C(5) alcohols in E. coli. Sci. Rep. 5, 11128.

Grund, A., Shapiro, J., Fennewald, M., Bacha, P., Leahy, J., Markbreiter, K., Nieder, M., Toepfer, M., 1975. Regulation of alkane oxidation in Pseudomonas putida. J. Bacteriol. 123, 546–556.
Gustavsson, M., Lee, S.Y., 2016. Prospects of microbial cell factories developed through systems metabolic engineering. Microb Biotechnol 9, 610–617.
Gusyatiner, M.M., Lunts, M.G., Kozlov, Y.I., Ivanovskaya, L.V., Voroshilova, E.B., 2002. DNA coding for mutant isopropylmalate synthase L-leucine-producing microorganism and method for producing L-leucine. U.S. Patent No. 6, 403,342.
Hammer, S.K., Zhang, Y., Avalos, J.L., 2020. Mitochondrial compartmentalization confers specificity to the 2-ketoacid recursive pathway: increasing isopentanol production in Saccharomyces cerevisiae. ACS Synth. Biol. 9, 546–555.
Hartigan, J.A., Wong, M.A., 1979. Algorithm AS 136: a k-means clustering algorithm. J. Roy. Stat. Soc. 28, 100–108.
Hazelwood, L.A., Daran, J.M., van Maris, A.J.A., Pronk, J.T., Dickinson, J.R., 2008. The Ehrlich pathway for fusel alcohol production: a century of research on Saccharomyces cerevisiae metabolism Appl. Environ. Microbiol. 74, 3920-3920.
Hillson, N., Caddick, M., Cai, Y., Carrasco, J.A., Chang, M.W., Curach, N.C., Bell, D.J., Le Feuvre, R., Friedman, D.C., Fu, X., Gold, N.D., Herrgard, M.J., Holowko, M.B., Johnson, J.R., Johnson, R.A., Keasling, J.D., Kitney, R.I., Kondo, A., Liu, C., Martin, V.J.J., Menolascina, F., Ogino, C., Patron, N.J., Pavan, M., Poh, C.L., Pretorius, I.S., Rosser, S.J., Scrutton, N.S., Storch, M., Tekotte, H., Travnik, E., Vickers, C.E., Yew, W.S., Yuan, Y., Zhao, H., Freemont, P.S., 2019. Building a global alliance of biofoundries. Nat. Commun. 10, 2040.
Jaspers, M.C., Meier, C., Zehnder, A.J., Harms, H., van der Meer, J.R., 2001. Measuring mass transfer processes of octane with the help of an alkSalkB::gfp-tagged Escherichia coli. Environ. Microbiol. 3, 512–524.
Jeschek, M., Gerngross, D., Panke, S., 2016. Rationally reduced libraries for combinatorial pathway optimization minimizing experimental effort. Nat. Commun. 7, 11163.
Jessop, P.G., 2016. The use of auxiliary substances (e.g. solvents, separation agents) should be made unnecessary wherever possible and innocuous when used. Green Chem. 18, 2577–2578.
Kapust, R.B., Tozser, J., Fox, J.D., Anderson, D.E., Cherry, S., Copeland, T.D., Waugh, D. S., 2001. Tobacco etch virus protease: mechanism of autolysis and rational design of stable mutants with wild-type catalytic proficiency. Protein Eng. 14, 993–1000.
Kelley, L.A., Mezulis, S., Yates, C.M., Wass, M.N., Sternberg, M.J., 2015. The Phyre2 web portal for protein modeling, prediction and analysis. Nat. Protoc. 10, 845–858.
Kok, M., Oldenhuis, R., van der Linden, M.P., Raatjes, P., Kingma, J., van Lelyveld, P.H., Witholt, B., 1989. The Pseudomonas oleovorans alkane hydroxylase gene. Sequence and expression. J. Biol. Chem. 264, 5435–5441.
Kurth, E.G., Doughty, D.M., Bottomley, P.J., Arp, D.J., Sayavedra-Soto, L.A., 2008. Involvement of BmoR and BmoG in n-alkane metabolism in 'Pseudomonas butanovora. Microbiology 154, 139–147.
Lamsen, E.N., Atsumi, S., 2012. Recent progress in synthetic biology for microbial production of C3-C10 alcohols. Front. Microbiol. 3, 196.
Lawson, C.E., Marti, J.M., Radivojevic, T., Jonnalagadda, S.V.R., Gentz, R., Hillson, N.J., Peisert, S., Kim, J., Simmons, B.A., Petzold, C.J., Singer, S.W., Mukhopadhyay, A., Tanjore, D., Dunn, J.G., Garcia Martin, H., 2021. Machine learning for metabolic engineering: a review. Metab. Eng. 63, 34–60.
Levin-Karp, A., Barenholz, U., Bareia, T., Dayagi, M., Zelcbuch, L., Antonovsky, N., Noor, E., Milo, R., 2013. Quantifying translational coupling in E. coli synthetic operons using RBS modulation and fluorescent reporters. ACS Synth. Biol. 2, 327–336.
Li, S., Wen, J., Jia, X., 2011. Engineering Bacillus subtilis for isobutanol production by heterologous Ehrlich pathway construction and the biosynthetic 2-ketoisovalerate precursor pathway overexpression. Appl. Microbiol. Biotechnol. 91, 577–589.
Lin, X., Fan, J., Wen, Q., Li, R., Jin, X., Wu, J., Qian, W., Liu, D., Xie, J., Bai, J., Ying, H., 2014. Optimization and validation of a GC-FID method for the determination of acetone-butanol-ethanol fermentation products. J. Chromatogr. Sci. 52, 264–270.
Lisa, M.N., Cvirkaite-Krupovic, V., Richet, E., Andre-Leroux, G., Alzari, P.M., Haouz, A., Danot, O., 2019. Double autoinhibition mechanism of signal transduction ATPases with numerous domains (STAND) with a tetratricopeptide repeat sensor. Nucleic Acids Res. 47, 3795–3810.
Liu, F., Wu, W., Tran-Gyamfi, M.B., Jaryenneh, J.D., Zhuang, X., Davis, R.W., 2017. Bioconversion of distillers' grains hydrolysates to advanced biofuels by an Escherichia coli co-culture. Microb. Cell Factories 16, 192.
Liu, Y., Nielsen, J., 2019. Recent trends in metabolic engineering of microbial chemical factories. Curr. Opin. Biotechnol. 60, 188–197.
Machas, M.S., McKenna, R., Nielsen, D.R., 2017. Expanding upon styrene biosynthesis to engineer a novel route to 2-phenylethanol. Biotechnol. J. 12.
Makart, S., Heinemann, M., Panke, S., 2007. Characterization of the AlkS/P(alkB)-expression system as an efficient tool for the production of recombinant proteins in Escherichia coli fed-batch fermentations. Biotechnol. Bioeng. 96, 326–336.
Mannan, A.A., Liu, D., Zhang, F., Oyarzun, D.A., 2017. Fundamental design principles for transcription-factor-based metabolite biosensors. ACS Synth. Biol. 6, 1851–1859.
Martinez-Garcia, E., Goni-Moreno, A., Bartley, B., McLaughlin, J., Sanchez-Sampedro, L., Pascual Del Pozo, H., Prieto Hernandez, C., Marletta, A.S., De Lucrezia, D., Sanchez-Fernandez, G., Fraile, S., de Lorenzo, V., 2020. Seva 3.0: an update of the Standard European Vector Architecture for enabling portability of genetic constructs among diverse bacterial hosts. Nucleic Acids Res. 48, D1164–D1170.
Mehrer, C.R., Rand, J.M., Incha, M.R., Cook, T.B., Demir, B., Motagamwala, A.H., Kim, D., Dumesic, J.A., Pfleger, B.F., 2019. Growth-coupled bioconversion of levulinic acid to butanone. Metab. Eng. 55, 92–101.
Miao, R., Xie, H., F, M.H., Lindblad, P., 2018. Protein engineering of alpha-ketoisovalerate decarboxylase for improved isobutanol production in Synechocystis PCC 6803. Metab. Eng. 47, 42–48.
Moreno, R., Marzi, S., Romby, P., Rojo, F., 2009. The Crc global regulator binds to an unpaired A-rich motif at the Pseudomonas putida alkS mRNA coding sequence and inhibits translation initiation. Nucleic Acids Res. 37, 7678–7690.
Morgan, S.A., Nadler, D.C., Yokoo, R., Savage, D.F., 2016. Biofuel metabolic engineering with biosensors. Curr. Opin. Chem. Biol. 35, 150–158.
Nguyen, N.P., Raynaud, C., Meynial-Salles, I., Soucaille, P., 2018. Reviving the Weizmann process for commercial n-butanol production. Nat. Commun. 9, 3682.
Nielsen, D.R., Leonard, E., Yoon, S.H., Tseng, H.C., Yuan, C., Prather, K.L., 2009. Engineering alternative butanol production platforms in heterologous bacteria. Metab. Eng. 11, 262–273.
Nissen, T.L., Kielland-Brandt, M.C., Nielsen, J., Villadsen, J., 2000. Optimization of ethanol production in Saccharomyces cerevisiae by metabolic engineering of the ammonium assimilation. Metab. Eng. 2, 69–77.
Nitschel, R., Ankenbauer, A., Welsch, I., Wirth, N.T., Massner, C., Ahmad, N., McColm, S., Borges, F., Fotheringham, I., Takors, R., Blombach, B., 2020. Engineering Pseudomonas putida KT2440 for the production of isobutanol. Eng. Life Sci. 20, 148–159.
Panke, S., Meyer, A., Huber, C.M., Witholt, B., Wubbolts, M.G., 1999. An alkane-responsive expression system for the production of fine chemicals. Appl. Environ. Microbiol. 65, 2324–2332.
Peralta-Yahya, P.P., Zhang, F., del Cardayre, S.B., Keasling, J.D., 2012. Microbial engineering for the production of advanced biofuels. Nature 488, 320–328.
Presnell, K.V., Alper, H.S., 2019. Systems metabolic engineering meets machine learning: a new era for data-driven metabolic engineering. Biotechnol. J. 14, e1800416.
Qian, S., Li, Y., Cirino, P.C., 2019. Biosensor-guided improvements in salicylate production by recombinant Escherichia coli. Microb. Cell Factories 18.
Reed, B., Blazeck, J., Alper, H., 2012. Evolution of an alkane-inducible biosensor for increased responsiveness to short-chain alkanes. J. Biotechnol. 158, 75–79.
Rogers, J.K., Taylor, N.D., Church, G.M., 2016. Biosensor-based engineering of biosynthetic pathways. Curr. Opin. Biotechnol. 42, 84–91.
Rojo, F., 2009. Degradation of alkanes by bacteria. Environ. Microbiol. 11, 2477–2490.
Salis, H.M., Mirsky, E.A., Voigt, C.A., 2009. Automated design of synthetic ribosome binding sites to control protein expression. Nat. Biotechnol. 27, 946–950.
Sambrook, J.F., Russel, D.W., 2001. Molecular Cloning: A Laboratory Manual. Cold Spring Harbor Laboratory.
Sayavedra-Soto, L.A., Doughty, D.M., Kurth, E.G., Bottomley, P.J., Arp, D.J., 2005. Product and product-independent induction of butane oxidation in Pseudomonas butanovora. FEMS Microbiol. Lett. 250, 111–116.
Schindelin, J., Arganda-Carreras, I., Frise, E., Kaynig, V., Longair, M., Pietzsch, T., Preibisch, S., Rueden, C., Saalfeld, S., Schmid, B., Tinevez, J.Y., White, D.J., Hartenstein, V., Eliceiri, K., Tomancak, P., Cardona, A., 2012. Fiji: an open-source platform for biological-image analysis. Nat. Methods 9, 676–682.
Sevilla, E., Yuste, L., Rojo, F., 2015. Marine hydrocarbonoclastic bacteria as whole-cell biosensors for n-alkanes. Microb Biotechnol 8, 693–706.
Sheppard, M.J., Kunjapur, A.M., Prather, K.L.J., 2016. Modular and selective biosynthesis of gasoline-range alkanes. Metab. Eng. 33, 28–40.
Sievers, F., Wilm, A., Dineen, D., Gibson, T.J., Karplus, K., Li, W., Lopez, R., McWilliam, H., Remmert, M., Soding, J., Thompson, J.D., Higgins, D.G., 2011. Fast, scalable generation of high-quality protein multiple sequence alignments using Clustal Omega. Mol. Syst. Biol. 7, 539.
Sticher, P., Jaspers, M.C., Stemmler, K., Harms, H., Zehnder, A.J., van der Meer, J.R., 1997. Development and characterization of a whole-cell bioluminescent sensor for bioavailable middle-chain alkanes in contaminated groundwater samples. Appl. Environ. Microbiol. 63, 4053–4060.
Straathof, A.J.J., Wahl, S.A., Benjamin, K.R., Takors, R., Wierckx, N., Noorman, H.J., 2019. Grand research challenges for sustainable industrial biotechnology. Trends Biotechnol. 37, 1042–1050.
Taylor, N.D., Garruss, A.S., Moretti, R., Chan, S., Arbing, M.A., Cascio, D., Rogers, J.K., Isaacs, F.J., Kosuri, S., Baker, D., Fields, S., Church, G.M., Raman, S., 2016. Engineering an allosteric transcription factor to respond to new ligands. Nat. Methods 13, 177–183.
Team, R.C., 2014. R: A Language and Environment for Statistical Computing. R Foundation for Statistical Computing, Vienna, Austria.
The 2007 OECD List of High Production Volume Chemicals, 2009. The 2007 OECD List of High Production Volume Chemicals.
Thorndike, R.L., 1953. Who belongs in the family. Psychometrika 18, 267–276.
van Beilen, J.B., Marin, M.M., Smits, T.H., Rothlisberger, M., Franchini, A.G., Witholt, B., Rojo, F., 2004. Characterization of two alkane hydroxylase genes from the marine hydrocarbonoclastic bacterium Alcanivorax borkumensis. Environ. Microbiol. 6, 264–273.
van Beilen, J.B., Panke, S., Lucchini, S., Franchini, A.G., Rothlisberger, M., Witholt, B., 2001. Analysis of Pseudomonas putida alkane-degradation gene clusters and flanking insertion sequences: evolution and regulation of the alk genes. Microbiology 147, 1621–1630.
van der Meer, J.R., Belkin, S., 2010. Where microbiology meets microengineering: design and applications of reporter bacteria. Nat. Rev. Microbiol. 8, 511–522.
Vogt, M., Brusseler, C., Ooyen, J.V., Bott, M., Marienhagen, J., 2016. Production of 2-methyl-1-butanol and 3-methyl-1-butanol in engineered Corynebacterium glutamicum. Metab. Eng. 38, 436–445.
Wang, C., Pfleger, B.F., Kim, S.W., 2017. Reassessing Escherichia coli as a cell factory for biofuel production. Curr. Opin. Biotechnol. 45, 92–103.
Yu, H., Chen, Z., Wang, N., Yu, S., Yan, Y., Huo, Y.X., 2019a. Engineering transcription factor BmoR for screening butanol overproducers. Metab. Eng. 56, 28–38.
Yu, H., Wang, N., Huo, W., Zhang, Y., Zhang, W., Yang, Y., Chen, Z., Huo, Y.X., 2019b. Establishment of BmoR-based biosensor to screen isobutanol overproducer. Microb. Cell Factories 18, 30.

Yuste, L., Rojo, F., 2001. Role of the crc gene in catabolic repression of the Pseudomonas putida GPo1 alkane degradation pathway. J. Bacteriol. 183, 6197–6206.
Zhang, J., Chen, Y., Fu, L., Guo, E., Wang, B., Dai, L., Si, T., 2021. Accelerating strain engineering in biofuel research via build and test automation of synthetic biology. Curr. Opin. Biotechnol. 67, 88–98.
Zhang, J.H., Chung, T.D., Oldenburg, K.R., 1999. A simple statistical parameter for use in evaluation and validation of high throughput screening assays. J. Biomol. Screen 4, 67–73.
Zhang, K., Sawaya, M.R., Eisenberg, D.S., Liao, J.C., 2008. Expanding metabolism for biosynthesis of nonnatural alcohols. Proc. Natl. Acad. Sci. U. S. A. 105, 20653–20658.
Zhao, J., Kardashliev, T., Joelle Ruff, A., Bocola, M., Schwaneberg, U., 2014. Lessons from diversity of directed evolution experiments by an analysis of 3,000 mutations. Biotechnol. Bioeng. 111, 2380–2389.
Zobel, S., Benedetti, I., Eisenbach, L., de Lorenzo, V., Wierckx, N., Blank, L.M., 2015. Tn7-Based device for calibrated heterologous gene expression in Pseudomonas putida. ACS Synth. Biol. 4, 1341–1351.